International Journal of Nanomedicine

Dovepress
Taylor & Francis Group

Open Access Full Text Article

ORIGINAL RESEARCH

Development of Solid Self-Nanoemulsifying Drug Delivery System of Rhein to Improve Biopharmaceutical Performance: Physiochemical Characterization, and Pharmacokinetic Evaluation

Sachin Madhusudan More[1,*], Md Abdur Rashid[2], Rohini S Kharwade[3,*], Murtada Taha[4], Yahya Alhamhoom[2], Gamal Osman Elhassan[5], Purushottam Gangane[3], Turky Omar Asar[6], Ajay Pise[7], Mohammed Kaleem[1], Md Ali Mujtaba[8,9]

[1]Department of Pharmacology, Dadasaheb Balpande College of Pharmacy, Rashtrasant Tukadoji Maharaj Nagpur University, Nagpur, MH, 440037, India; [2]Department of Pharmaceutics, College of Pharmacy, King Khalid University, Abha, Saudi Arabia; [3]Department of Pharmaceutics, Dadasaheb Balpande College of Pharmacy, Rashtrasant Tukadoji Maharaj Nagpur University, Nagpur, MH, 440037, India; [4]Department of Clinical Laboratory Science, Prince Sultan Military College of Health Sciences, Dhahran, Saudi Arabia; [5]Department of Pharmaceutics, College of Pharmacy, Qassim University, Buraidah, Saudi Arabia; [6]Department of Biology, College of Science and Arts at Alkamil, University of Jeddah, Jeddah, Saudi Arabia; [7]Department of Regulatory Affairs Dadasaheb Balpande College of Pharmacy, Rashtrasant Tukadoji Maharaj Nagpur University, Nagpur, MH, 440037, India; [8]Department of Pharmaceutics, Faculty of Pharmacy, Northern Border University, Arar, Saudi Arabia; [9]Center for Health Research, Northern Border University, Arar, Saudi Arabia

* These authors contributed equally to this work

Correspondence: Md Ali Mujtaba; Mohammed Kaleem, Email m.mujtaba@nbu.edu.sa; kaleemmubin88@gmail.com

Introduction: Rhein, a natural bioactive lipophilic compound with numerous pharmacological activities, faces limitations in clinical application due to poor aqueous solubility and low bioavailability. Thus, this study aimed to develop a rhein-loaded self-nano emulsifying drug delivery system (RL-SNEDDS) to improve solubility and bioavailability.

Methods: The RL-SNEDDS was prepared by aqueous titration method with eucalyptus oil (oil phase), tween 80 (surfactant), and PEG 400 (co-surfactant) and optimization was performed by 3^2 factorial design. The optimized formulation was characterized for Fourier transform infrared spectroscopy, differential scanning calorimetry, powdered X-ray diffraction, and Field emission scanning electron microscopy. Further, the oral bioavailability study and brain tissue pharmacokinetics study were performed on Sprague-Dawley rats.

Results: The optimized RL-SNEDDS had an average droplet size of 129.3 ±1.57 nm, zeta potential of −24.6 mV ±0.34, % transmittance of 94.82 ± 0.61, and encapsulation efficiency of 98.86 ± 0.23. Furthermore, RL-SNEDDS was transformed into solid RL-SNEDDS (RS-SNEDDS) to increase stability. In vitro release of rhein from RS-SNEDDS showed prolonged release up to 24h with 99.03± 1.04% drug release. Differential scanning calorimetry and powdered X-ray diffraction analysis confirmed the reduction in drug crystallinity and supported the results of the dissolution study. Field emission scanning electron microscopy analysis revealed the smooth and spherical nanosized globule of SNEDDS. Moreover, the in vivo pharmacokinetic study showed a significantly higher ($p \leq 0.05$) value of C_{max} and AUC_{0-t} of RS-SNEDDS (8 ± 0.930 µg/mL and 37.79 ± 2.01 µg/mL*hr) compared to free rhein suspension (1.96 ± 0.712 µg/mL and 7.32 ± 0.946 µg/mL*hr) which indicated the enhancement of bioavailability of RS-SNEDDS. We also examined the C_{max} and AUC_{0-t} of RS-SNEDDS in the brain and it was found to be 2.90 ± 0.171 µg/mL and 18.18 ± 1.68 µg/mL*hr respectively.

Conclusion: This study concludes that the RS-SNEDDS improves brain tissue concentration and oral bioavailability, both of which increase therapeutic potential.

Keywords: rhein, bioavailability, solubility, nanoemulsion, drug release, pharmacokinetic

Received: 2 October 2024
Accepted: 18 December 2024
Published: 7 January 2025

Graphical Abstract

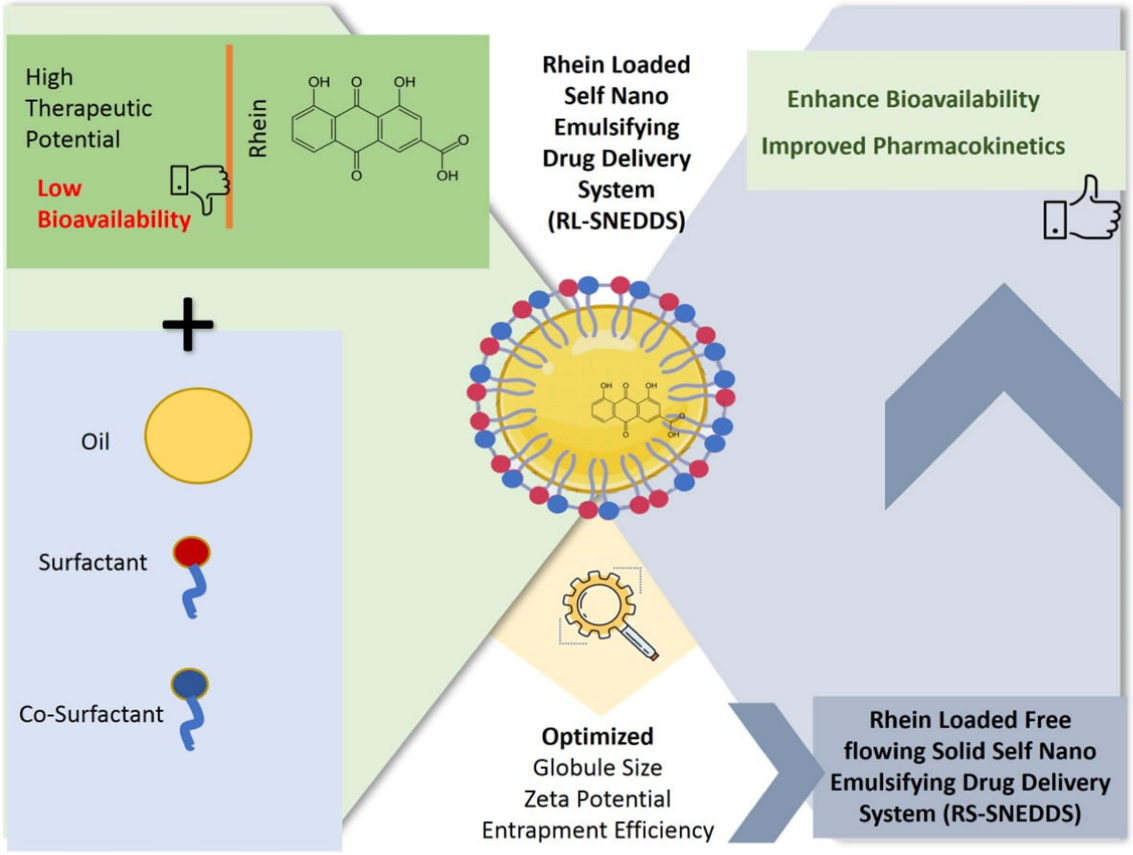

Introduction

Rhein (4,5-dihydroxyanthraquinone-2-carboxylic acid) is a naturally occurring lipophilic anthraquinone derivative and principally obtained from the rhizomes of the rheum species, also known as rhubarb.[1] It contains two hydroxyl groups and one carboxyl group and has strong polarity and electrochemical redox properties. Rhein exhibits many pharmacological effects, including hepatoprotective, anti-fibrosis, nephroprotective, anti-inflammatory, antioxidant, anticancer, lipid-lowering, and antimicrobial activities.[1–3] Because of its many therapeutic uses, rhubarb has been utilized for many years as a traditional medicine in China. The poor aqueous solubility of rhein hampers its broader applications. Furthermore, out of all anthraquinone, only rhein (log P value = 2.86) would be able to pass the blood–brain barrier. However, its poor water solubility is considered a biopharmaceutical classification system class II; therefore, its absorption and oral bioavailability are limited due to its poor aqueous solubility.[4] Therefore, it is essential to develop and optimize a novel formulation that can raise the bioavailability of rhein and finally, enhance its therapeutic potential.

Nowadays, the poor water solubility of novel pharmacological entities is one of the most significant challenges in the field of biomedical science, which presents a major obstacle for pharmaceutical scientists.[5] Oral bioavailability could be improved through multiple types of formulation techniques, such as solid dispersions, permeation enhancers, gastroprotective systems, nanosuspensions, surfactants, and, lipid-based formulations.[6] The main challenge in developing delivery systems is the poor water solubility of drugs. Before being absorbed into the systemic circulation, the drug must be able to dissolve in the gastrointestinal fluid to have adequate bioavailability when taken orally. Various studies have reported several nanoformulations of rhein to improve oral bioavailability. Yao et al used deoxycholic acid-

conjugated rhein nanoparticles (NPs) to improve oral bioavailability.[7] Feng et al prepared rhein-loaded solid lipid NPs by heat homogenization followed by ultrasonication, and the results showed that the solid lipid NPs formulation of rhein had higher oral absorption and improved oral bioavailability.[8] Luo, J. et al prepared Rhein conjugates with low molecular weight chitosan to improve solubility and bioavailability. The results showed that rhein-chitosan conjugates increased seven-fold $T_{1/2}$ and 3.1-fold $AUC_{0-\infty}$ as compared to suspension formulation.[9]

To increase the solubility and bioavailability of weakly water-soluble substances, a variety of delivery methods, such as lipid-based delivery systems, have been used.[10] Lipid-based formulations are promising approaches to enhance water solubility and the dissolution rate. Self-nano-emulsifying drug-delivery systems (RL-SNEDDS) are among the several lipid-based drug-delivery systems that have been studied extensively for oral drug delivery. RL-SNEDDS is an isotropic homogenous mixture of oils, surfactants, co-solvents, and drugs that produces spontaneously a nano-emulsion when diluted with water and agitated gently. It occurs by modifying the entropy, favoring the dispersion process, and increasing the surface area.[11] This approach increases the solubility and increases the rate of absorption of insoluble pharmaceuticals by encapsulating the insoluble lipophilic drug in a dissolved form that is comparatively smaller than 200 nm. In addition to potentially improving the delivery of insoluble drugs, RL-SNEDDS also has the potential to offer improved enzymatic and chemical stability, a wider interfacial area for absorption, and increased oral bioavailability after administration.[12,13] RL-SNEDDS formulations are often liquid formulations, also referred to as Liquid-SNEDDS (RL-SNEDDS). However, RL-SNEDDS has some limitations, such as stability, portability, and undesirable interactions with excipients as well as capsule shells. Hence, to address these problems, RL-SNEDDS has been converted to solid RL-SNEDDS (RS-SNEDDS) , comprising water-soluble solid carriers by lyophilization or spray drying techniques by removing water from RL-SNEDDS.[7] Lyophilized RS-SNEDDS had better particle size, rate of dissolution, stability, and flow properties than spray-dried ones, which extends its applications.[8]

There are currently no reports from the literature on the development of rhein-loaded RS-SNEDDS to improve oral bioavailability. In this work, rhein, a bioactive substance, was added to RL-SNEDDS to solve the solubility issue. Therefore, this study aimed to develop and optimize rhein-loaded RS-SNEDDS to increase the oral bioavailability of rhein, assess the physicochemical properties, and evaluate its pharmacokinetic along with the determination of brain tissue concentration, which facilitates its neuroprotective treatment response.

Materials and Methods

Materials

Rhein and Diacerein were obtained from Alembic Pharmaceuticals Ltd, Gujarat India. Orthophosphoric acid, acetonitrile, and methanol (HPLC grade) were purchased from Loba Chemie Pvt. Ltd. Mumbai, India. Eucalyptus oil, tween 80, PEG 200, and mannitol had been procured from Sisco Research & Lab Pvt. Ltd. Mumbai, India. The remaining chemicals and reagents were of analytical grade.

Solubility Analysis of Rhein

The components of RL-SNEDDS were selected based on solubility analysis of the drug in several surfactants, co-surfactants, and oils. Therefore, the solubility of rhein was determined in oils (Arachis Oil, Castor Oil, Cotton seed oil, Ethyl oleate, and Eucalyptus oil), surfactants (Tween 80, Tween 20, Span 80, and Kolliphor EL) and co-surfactants (Propylene glycol, Polyethylene glycol (PEG) 400 and Span 20). Initially, an excess quantity of rhein (100 mg) in different glass vials was placed and separately added 1 gram of each component in the vials. All vials were closed and mixed using a vortex mixer (Remi Motors, Pvt. Ltd., India) for 10–15 min to facilitate solubilization. Further, all mixtures were shaken on a mechanical shaker for 48 hours at 37 ± 2°C to reach equilibrium. After equilibration, the samples were centrifuged for 15 minutes at 5000 rpm. The supernatant was withdrawn and the content of rhein was measured using high-performance liquid chromatography (HPLC) at 250 nm.[9] The experiments were done in triplicate. The excipient that exhibited the highest solubility of rhein was chosen to construct the pseudo-ternary phase diagram.

Construction of Pseudo-Ternary Plot

To optimize the quantities of oil, surfactant, and co-surfactant and determine their mixing ratios, pseudo-ternary phase diagrams were created to identify the nanoemulsion zone. The oil phase, surfactant, and cosurfactant were selected based on the highest solubility of rhein for the construction of a pseudo-ternary phase diagram using the aqueous titration method.[10] For each phase diagram, the surfactant: cosurfactant (S_{mix}) was selected in a ratio of 1:1, 2:1, 3:1, and 4:1. Each S_{mix} ratio was blended with oil in a ratio of 1:9 to 9:1 in separate glass vials with a 50 rpm stirring speed. Each weight ratio of oil and S_{mix} was titrated gradually with water and visual observation was done to determine the phase clarity. Pseudo-ternary phase diagrams were plotted using Chemix School 3.50 trial edition software. The S_{mix} ratios and component ratios of the S_{mix} mixtures with oil that produced nanoemulsions (transparent and clear mixtures) were chosen.

Optimization of Formulation Using Experimental Design

Many formulation-related parameters influenced the self-emulsification ability of RL-SNEDDS, including surfactant concentration, oil/S_{mix} ratio, droplet size (DS), emulsification time (ET), %transmittance (%T), and zeta potential (ZP). Therefore, the RL-SNEDDS formulation was formulated by optimizing the quantitative relations between two independent variables: the oil concentration and S_{mix} (3:1). To optimize the levels of variables in the RL-SNEDDS formulations, a 3^2 full factorial experimental design was used. 3^2 factorial designs with two variables, including eucalyptus oil (X_1) concentration and optimized S_{mix} (X_2), were considered as shown in Table 1. These two factors varied at three levels. The effect of independent variables (X_1 and X_2) on dependent variables: DS (Y_1), % T (Y_2), and ET (Y_3) were examined. Optimization of formulation variables, experimental runs, and ANOVA analysis was performed using Design-expert software version 13 (Stat-Ease, Inc. Minneapolis, MN).[14,15]

Formulation of Rhein-Loaded RL-SNEDDS

3^2 full factorial design was used and a total of 10 RL-SNEDDS prototype formulations were prepared. Ten milligrams of rhein was added in eucalyptus oil to each formulation. The specified concentration of S_{mix} was thoroughly mixed using a vortex mixture. Furthermore, all prepared batches were warmed to 40°C for 30 minutes while continuously shaking them and then cooled to room temperature.[12,14] These formulations were evaluated for various parameters like ET, DS, % T, ZP, %drug loading (%DL), and %entrapment efficiency (%EE).

Evaluation of Rhein-Loaded RL-SNEDDS

ET, %T, DS, PDI, and ZP Determination

ET was determined by visual observation. For this, 0.1 mL RL-SNEDDS formulation was diluted to 100 mL of 0.01 M phosphate buffer (pH 6.8). It was mixed gently with a magnetic stirrer at 37 ± 5°C and noted the time for the formation of clear and transparent emulsion. For the determination of %T, the diluted dispersion of RL-SNEDDS formulations was scanned and transmittance was recorded at 630 nm in a zeta sizer instrument (Anton-Paar Litesizer-500, Austria).[16] The DS and polydispersity index (PDI) were determined by the dynamic light scattering method. The ZP

Table 1 Independent and Dependent Variables in 3^2 Factorial Design

Independent Variables	**Levels**		
	Low (−1)	**Medium (0)**	**High (+1)**
X_1= Concentration of oil (mL)	0.50	0.55	0.60
X_2=Concentration S_{mix}(mL)	0.40	0.45	0.50
Concentration of rhein (mg)	10	10	10
Dependent Variables: Y_1: Droplet size, Y_2: % transmittance, and Y_3: emulsification time			

was determined by the electrophoretic light scattering method. Each formulation batch was evaluated for DS, PDI, and ZP using a zeta sizer instrument (Anton-Paar Litesizer-500, Austria).[10] Each experiment was replicated three times.

% DL Determination

Rhein-containing RL-SNEDDS (equivalent to 10 mg rhein) formulation was dissolved in 25 mL of methanol and sonicated for 15 min. Further, it was centrifuged at 2000 rpm for 15 minutes and then filtered using a membrane filter to separate the supernatant. Subsequently, 1 mL of filtrate was then diluted using methanol. The diluted filtrate was analyzed using HPLC at 250 nm.[9]

$$\%\ \text{Drug loading} = \frac{\text{Practical drug content detected}}{\text{Theoretical drug content added}} \text{x}100 \quad (1)$$

%EE Determination

Rhein-loaded RL-SNEDDS (equivalent to 10 mg rhein) was centrifuged at 10,000 rpm for 15 mins to separate unencapsulated rhein. The aliquot of the solution was filtered, diluted with methanol, and analyzed by HPLC to determine the quantity of free rhein.[17] The % EE was determined by using the following formula:

$$\%\ \text{Encapsulation Efficiency} = \frac{\text{Weight of total rhein added into SNEDDE} - \text{Weight of free rhein}}{\text{Weight of total rhein added into SNEDDE}} \text{x}100 \quad (2)$$

Preparation of Solid RL-SNEDDS (RS-SNEDDS) by Lyophilization

The optimized batch of rhein-loaded RL-SNEDDS was converted to more stable and free-flowing powder with the help of mannitol as a cryoprotectant carrier. The optimized batch of rhein-loaded RL-SNEDDS and mannitol was taken in a 2:1 w/w ratio. 10 gm of RL-SNEDDS was dissolved in 100 mL distilled water by gentle stirring at 100 rpm for 10 min. Further, 5 gm of mannitol was added to it and stirred for 10 mins. The suspension was freeze-dried by lyophilizer (MAC Lyophilizer, Cat. No: MSW-137) at condenser temperature −60°C with pressure below 15 Pascal and converted to free-flowing rhein-loaded Solid RL-SNEDDS (RS-SNEDDS).[18]

Solid State Characterization of RS-SNEDDS

Fourier Transform Infrared Spectroscopy (FTIR) Analysis

Rhein, mannitol, and RS-SNEDDS of rhein were characterized by FTIR for determining the compatibility of rhein with excipients. It was carried out by using the KBr disk method with a scanning range of 400 to 4000cm^{-1} using a Shimadzu FTIR spectrometer (Shimadzu Corporation, Kyoto, Japan).[19]

Differential Scanning Calorimetry (DSC) Analysis

Rhein and RS-SNEDDS were also characterized by DSC (DSC-PYRIS-1, PerkinElmer, USA) to determine the phase transition of rhein. Accurately weighted 5mg of each sample was sealed in an aluminum pan and equilibrated at 25°C. It was then heated with a heat rate of 10°C/min over a wide range of 50°C to 300°C.[20]

Powdered X-Ray Diffraction (PXRD) Analysis

Rhein and RS-SNEDDS were evaluated for PXRD analysis at room temperature. The study was performed by XRD (Bruker D8 Advance, WI, USA) with Ni-filtered and Xe-filled proportional counters detectors under continuous mode with a scanning rate of 2°/min.[10]

Field Emission Scanning Electron Microscopy (FE-SEM) Analysis

FE-SEM (S-4100, Hitachi, Japan) was used to characterize the morphology along with the shape and size of RS-SNEDDS. The samples were placed on a standard copper grid covered in carbon-coating. Images were taken under a vacuum with an acceleration voltage of 200kV.[19]

 https://doi.org/10.2147/IJN.S499024

In vitro Dissolution Study and Release Kinetic

The cumulative % release of rhein through RS-SNEDDS and free rhein was determined using a USP type-II dissolution apparatus. The RS-SNEDDS and free rhein equivalent to 10 mg were separately placed inside the "0" size hard gelatin capsule. The capsule was placed in a dissolution beaker with 900 mL of acetate buffer (0.01M, pH 4) and phosphate buffer (0.01M, pH 6.8) at 37°C and 50 rpm rotation speed. Five-milliliter aliquots were then taken out at 5, 10, 20, 30, 60, and 120 min intervals, which were filtered and HPLC analysis was performed at 250 nm. The fresh dissolution medium was replaced to maintain the sink condition. The dissolution results were fitted in various kinetic models such as zero-order, first-order, Higuchi, Hixon-Crowell, and Korsmeyer-Peppas models and calculated the drug release exponent (n) to determine the drug release mechanism.[21–23]

In vivo Oral Bioavailability Study and Brain Tissue Pharmacokinetics

Study Protocol

Oral bioavailability study and brain tissue pharmacokinetics of optimized RL-SNEDDS formulation were performed on male Sprague-Dawley rats weighing 200–250g. This study was performed as per the guidelines approved by the Institutional Animal Ethics Committee (IAEC) of Dadasaheb Balpande College of Pharmacy, Nagpur, India with approved protocol number DBCOP/IAEC/1426/2022-23/P11. The animals were kept at 22 ±2°C and accessed standard laboratory food with water for one week before the experimentation. They were fasted overnight before starting the experiment.

Eighteen Sprague-Dawley male rats were used to evaluate in vivo bioavailability and brain tissue distribution pharmacokinetic characteristics. All rats were arbitrarily segregated into two groups, comprising free rhein group (n = 6) as group I, and optimized RL-SNEDDS formulation (n = 6) as group II. Group 1 received rhein suspension, while group 2 received RL-SNEDDS formulation with the dose of 10 mg/kg of body weight by oral route and group 3 was kept as a blank group without treatment.[24,25] Each group was housed independently in cages in a lab environment. The blood was taken at various time intervals, and the collected samples were stored in heparinized microcentrifuge tubes. This collected blood sample was centrifuged for 10 min at 12000 rpm at 4°C. The plasma was separated and transferred to the Eppendorf tube and stored at −20°C until further analysis. The plasma samples must be at room temperature before analysis and then subjected to single-step protein precipitation and investigated using the validated HPLC method at 250 nm.[26] The rats were sacrificed by cervical dislocation, and their brains were removed. Furthermore, we carefully homogenized the collected brain tissues, performed single-step protein precipitation, and determined the drug concentration in the brain tissue by running RP-HPLC at 250 nm.[24]

Sample Preparation and Bioanalytical Method Development and Validation for Rhein

Initially, the diacerein was selected as an internal standard (IS) for bioanalytical estimation of rhein based on close pKa value (3.0 for diacerein and 4.2 for rhein) and structural similarity of the anthraquinone group. A stock solution of rhein and IS with a concentration of 100 µg/mL was prepared in methanol. Working stock solutions of rhein in the range of 10 ng–100 ng/mL and IS 1 µg/mL were prepared from the above stock solution. The blood samples were withdrawn from the retro-orbital route and stored in an EDTA blood collection tube (Himedia Laboratory, Mumbai, India) for analysis. Further, it separately proceeded for the single-step protein precipitation using all concentrations of working stock solutions from rhein and IS through liquid–liquid extraction.[12,27]

The RP-HPLC (LC-20 AD Shimadzu, Japan) method development trials were performed using a detector based on photodiode arrays in the C18 Shimpack column (250 mmX4.6 mm,5µm). Analysis was carried out in isocratic mode employing an aqueous solution of orthophosphoric acid at various pH 3 and 4 (pump A), and acetonitrile was used for pump B. The trials were performed by varying the pump A:B ratio from 40:60, 45:55, and 50:50. The flow rate was changed from 0.6 to 1.0 mL/min to resolve the rhein peak from IS. A 0.2 µm membrane filter was used (Millipore, Bedford, MA, made in the USA) to filter all working solutions and the mobile phase. The sample injection of 20 µL was used for the RP-HPLC bioanalysis.[28]

The bioanalytical method was validated to ensure the reliability and acceptable performance of analytical results, including linearity, lower limit of detection (LOD), quantification (LOQ), system appropriateness, selectivity/specificity, matrix effect, and recovery study of analytes in the plasma. Six replicate injections of rhein (10µg/mL) with IS (1 µg/mL) spiked with the biological matrix were used to assess system suitability. The system suitability study was evaluated by analyzing retention time, resolution factor, capacity factor, number of theoretical plates, height equivalence of a theoretical plate (HETP), and the tailing factor of the chromatographic peaks of the analytes.[29] Linearity was examined at the concentration range from 1 µg/mL to 5µg/mL in the plasma. The samples were tested in triplicate with IS 1µg/mL.

A linear regression analysis of the area ratio (analyte/IS) vs concentration was plotted. The LOD and LOQ were computed as the lowest concentrations at which an analyte's peak height should be three and ten times the baseline noise, respectively.[30] The matrix effect and recovery were calculated at three concentration ranges: low (0.05 µg), medium (0.5 µg), and high (5 µg) using three replications. The extraction recovery was calculated using the peak area ratios of the biological matrix spiked before and after centrifugation with the rhein sample.[31,32]

Pharmacokinetic Parameters

Pharmacokinetic parameters were determined using the non-compartmental method with PK solver software. Various pharmacokinetic parameters and drug concentration in the brain tissues were determined individually, and the results are presented as mean ± SD.

Statistical Analysis

Graph Pad Prism Version-5 (Graph-Pad-Software, INC., La Jolla, CA, USA) was used for statistical analysis. To determine the standard deviation, all studies were performed in a triplicate and represented as mean ± SD.

Results and Discussion

Screening of RL-SNEDDS Components

The components of RL-SNEDDS were selected based on saturation solubility analysis of rhein in oils, surfactants, and cosurfactants. To improve the solubility of rhein and %DL, it is important to choose appropriate oils, surfactants, and cosurfactants while formulating the RL-SNEDDS. To prepare a stable formulation, the ingredients in RL-SNEDDS should maximize drug solubility and have good miscibility.[13] The solubility of rhein in different oils, surfactants, and co-surfactants was estimated and shown in Table 2. The drug's solubility in the oil phase is an important factor in the nanoemulsions formulation to keep the drug in its solubilized form. Eucalyptus oil showed the highest rhein solubility (12.53 mg/mL) as compared to other oils. Therefore, eucalyptus oil was chosen for the formulation of RL-SNEDDS as an oil phase. Different surfactants and cosurfactant types were used to assess the solubility of rhein. In surfactant, tween-80 showed the maximum solubility of rhein (17.61 mg/mL), and, in co-surfactant, the highest solubility was determined in PEG-400 (18.65 mg/mL) as shown in Table 2. The results showed that the hydrophilic–lipophilic balance (HLB) of surfactant determined the solubilizing ability of rhein. High HLB surfactants offered the benefit of rhein solubilization. The pseudo-ternary phase diagrams were plotted for varying concentrations of eucalyptus oil, PEG-400, and tween 80 to optimize the RL-SNEDDS formulation.

Table 2 Solubility of Rhein in Different Oils, Surfactants, and Co-Surfactants

S.No	Oils	Solubility(mg/mL)
1	Arachis Oil	1.05
2	Castor Oil	1.812
3	Cotton seed oil	2.940
4	Ethyl oleate	8.23
5	Eucalyptus oil	12.53
S.No	**Surfactants**	**Solubility(mg/mL)**
1	Tween 80	17.61
2	Tween 20	10.16
3	Span 80	8.07
4	Kolliphor EL	7.12
S.No	**Co-surfactants**	**Solubility(mg/mL)**
1	Propylene glycol	9.082
2	Polyethylene glycol (PEG) 400	18.65
3	Span 20	6.075

https://doi.org/10.2147/IJN.S499024

Construction of Pseudo-Ternary Phase Diagram

Ternary phase diagram plotting allowed us to explore the nano-emulsion region. Additionally, the ranges of concentration for eucalyptus oil, PEG-400, and tween 80 were determined. Initially, all formulations were made in the absence of rhein. The phase diagram was constructed by titrating all formulations with water observing opaqueness and turbidity. The area of the nano-emulsion region changed as the ratio of S_{mix} was changed from 1:1 to 4:1. The yellow-shaded portion in Figure 1 represented the homogeneous phase, whereas the non-shaded portion represented the biphasic region. The S_{mix} ratios 3:1 and 4:1 showed higher monophasic regions as compared to the S_{mix} ratios 1:1 and 2:1. The assessment of the emulsification time is used to determine the emulsification efficiency. It visually observed the time duration required to completely disperse the RL-SNEDDS in 100 mL water under mild agitation.[33] It is noteworthy that oil concentrations 0.5–0.6 with a S_{mix} (3:1) concentration range 0.4–0.5 of 3:1 showed the least amount of emulsification time and displayed a clear, transparent appearance with a little bluish tint (Grade A) as compared to other S_{mix} ratios. Therefore,

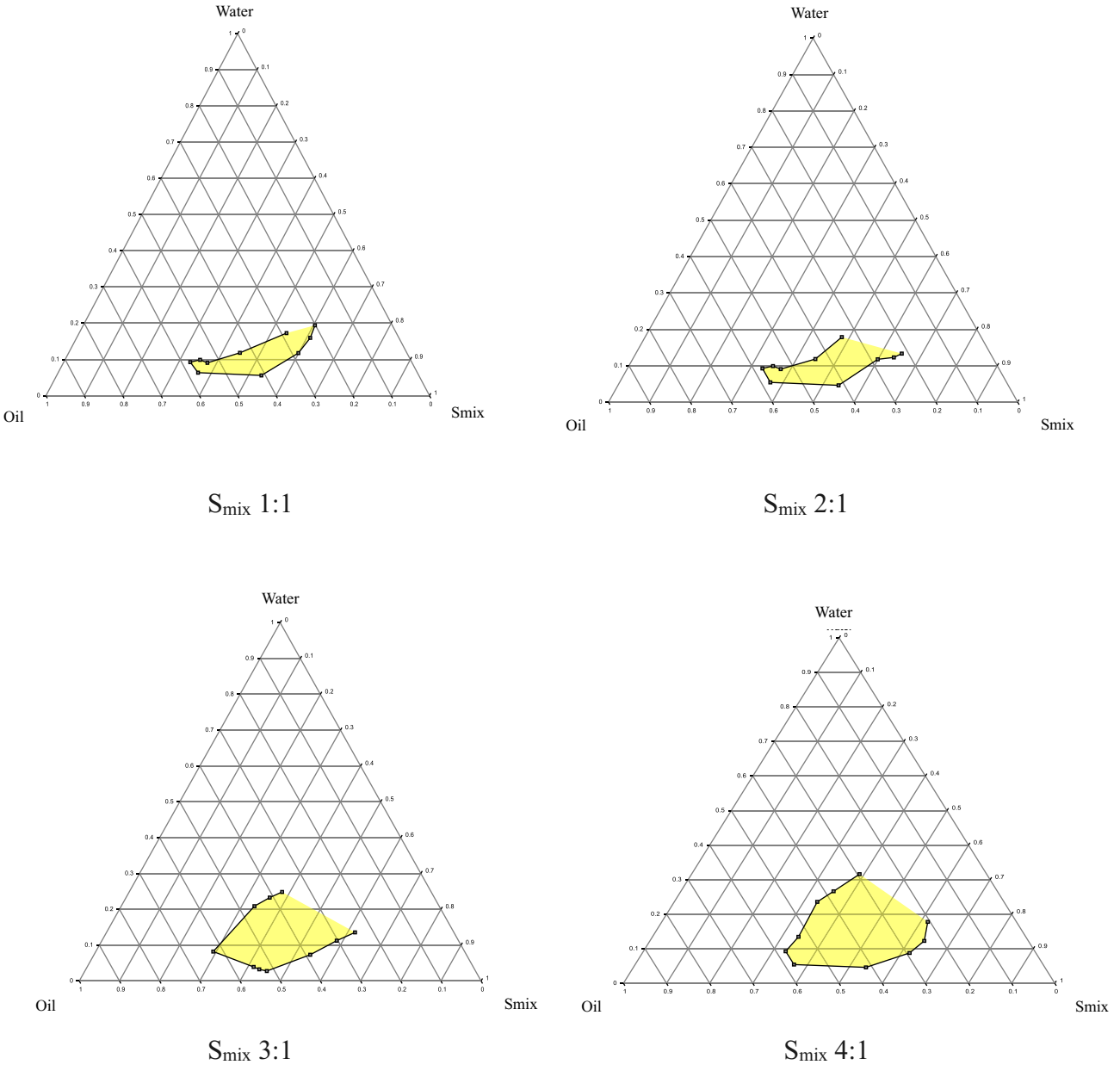

Figure 1 Pseudo ternary plot for assessing the nano-emulsion region of RL-SNEDDS and evaluating the surfactant: cosurfactant (S_{mix}) at different ratios of 1:1, 2:1, 3:1 and 4:1.

S_{mix} 3:1 from concentration 0.4–0.5 mL and oil concentration range 0.5–0.6 mL were selected for designing and optimizing the RL-SNEDDS formulation.

Formulation and Optimization of Rhein-Loaded RL-SNEDDS

From the pseudo ternary plot, the ratio of S_{mix} (3:1) in concentration 0.4–0.5 mL and eucalyptus oil concentration range 0.5–0.6 mL was selected as an independent variable for experimental design to optimize the RL-SNEDDS. 3^2 factorial design was used for the optimization of RL-SNEDDS formulation because it is the most efficient process for screening and determining suitable components for RL-SNEDDS. Also, this method has an advantage over other methods in that not only numerical factors but categorical factors like types of oil, surfactant, and co-surfactant could be examined.[34] The batches of RL-SNEDDS were designed by optimizing two separate parameters including the eucalyptus oil concentrations and S_{mix}. All formulated batches were evaluated for the response of DS, % T, and ET to optimize the RL-SNEDDS. In addition to this, all batches were also evaluated for % DR and % EE as illustrated in Table 3. The second-order polynomial equations with positive and negative sign terms confirmed the favorable and inverse relation between the concentration of eucalyptus oil and S_{mix} with all responses.

Effect of X_1 and X_2 on DS

The DS of RL-SNEDDS formulation is important as it affects drug release characteristics and absorption. The mean DS of all formulated batches (F1 – F10) was found within the range of 129.3 ± 1.57 nm to 153.2 ± 2.17 nm as shown in Table 3. The obtained polynomial equation 3 for DS followed the quadratic model with adjusted and the predicted R^2 value was near about one, and the P value was 0.05 for the. It revealed that DS is substantially affected by the interaction terms X1X2 and X_2^2. The interaction term X_1 greatly synergistically increases mean droplet size and the mean DS is significantly antagonized by polynomial terms X1X2, X_1^2 and X_2^2. From the result of the response plot and contour plot, the DS of RL-SNEDDS showed significant change concerning the concentration of eucalyptus oil. However, the concentration of S_{mix} showed an inverse relationship with DS as shown in Figure 2. Since S_{mix} covers the surface area of bioactive rhein-loaded oil globules and reduces the interfacial tension. The S_{mix} concentration also helps to increase the solubility of the drug and dispersibility of globules, thus promoting formulation homogeneity and stability.[35]

Table 3 Evaluation Parameters of RL-SNEDDS Formulation in 3^2 Factorial Designs

Independent variables Dependent variables								
Formulation Code	**X_1: Conc. of eucalyptus oil (mL)**	**X_2: Conc of S_{mix} (3:1) (mL)**	**DS (nm)**	**% T**	**Emulsification time (Sec)**	**% DL**	**%EE**	**ZP**
F1	0.6	0.45	153.2±2.17	91.12±0.92	54±1	98.04±0.28	96.65±0.95	−10.72±1.43
F2	0.6	0.4	147.7±1.78	89.52±0.82	61±1	97.73±0.33	97.03±0.67	−18.37±1.82
F3	0.5	0.4	136.2±2.61	93.30±0.69	46±2	99.07±0.16	98.14±0.81	−23.65±1.04
F4	0.6	0.5	144.1±0.94	88.12±0.81	44±1	97.45±0.68	96.05±0.72	−20.18±0.78
F5	0.55	0.45	151.5±2.05	91.10±0.85	50±1	98.15±0.42	97.35±0.69	−11.03±1.72
F6	0.55	0.45	150.9±0.92	92.87±0.94	55±1	98.21±0.71	97.68±0.47	−7.81±0.89
F7	0.5	0.5	129.3±1.57	94.82±0.61	42±2	98.86±0.23	97.74±0.72	−24.61±0.34
F8	0.55	0.4	148.1±1.68	87.53±0.87	58±1	98.11±0.51	96.89±0.64	−23.08±2.62
F9	0.5	0.45	145.6±1.92	94.81±0.73	38±2	98.36±0.38	97.67±0.71	−20.71±0.91
F10	0.55	0.5	149.2±1.43	88.93±0.68	59±1	97.85±0.41	96.36±0.64	−12.56±0.84

Note: All values are represented as mean ± SD (n = 3).

https://doi.org/10.2147/IJN.S499024

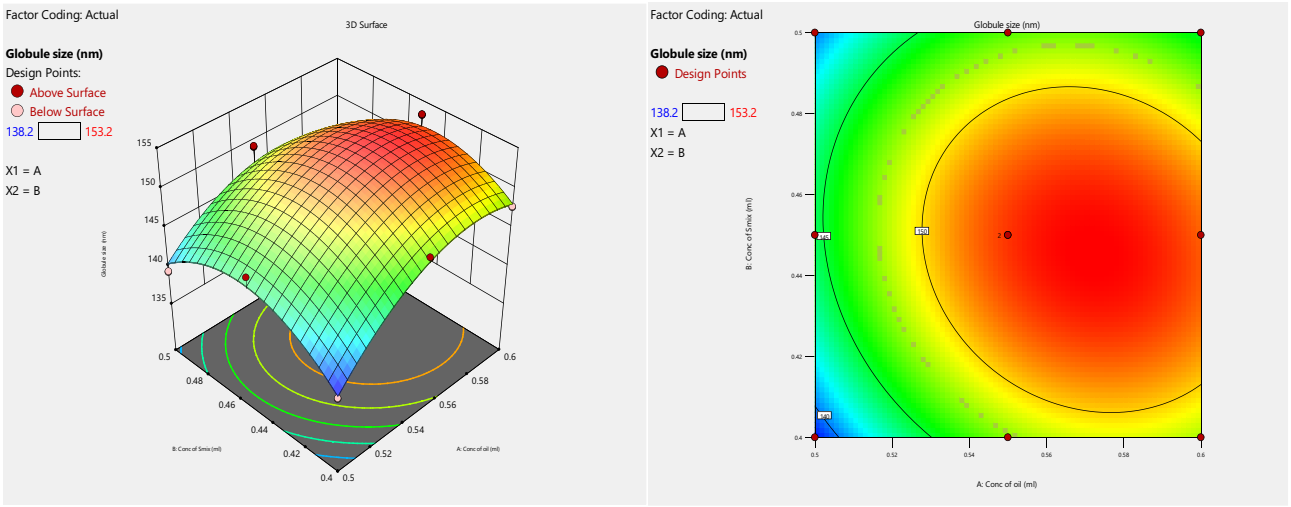

(a) (b)

Figure 2 (**a**) 3D response graph and (**b**) contour plot for the effect of concentration of eucalyptus oil and surfactant: cosurfactant (S_{mix}) on droplet size showed that the concentration of eucalyptus oil greatly increases mean droplet size however, the concentration of S_{mix} showed an inverse relationship with droplet size.

$$Y_1(DS) = 152.49 + 3.65X_1 - 0.2333X_2 - 1.17X_1X_2 - 4.39{X_1}^2 - 5.14{X_2}^2 \quad (3)$$

Effect of X_1 and X_2 on %T

The % T was selected as the second dependent response variable to optimize the rhein-loaded RL-SNEDDS. The 3D response plot and contour plot showed that as S_{mix} concentration raised, the %T also rose and decreased as the eucalyptus oil concentration increased as shown in Figure 3. Polynomial equation 4 also predicted the effect of eucalyptus oil and S_{mix} on %T. It also designates the quadratic interactive models with adjusted and the predicted R^2 value was near about one for the %T. From, the P value 0.05 in ANOVA the interaction terms X_1 X_2 have a non-significant effect. Factors ${X_1}^2$, and ${X_2}^2$ have a significant antagonistic effect on %T. Thus, it can be concluded that %T was increased with the increase in the concentration of S_{mix} and decreased along with an increase in the concentration of oil.

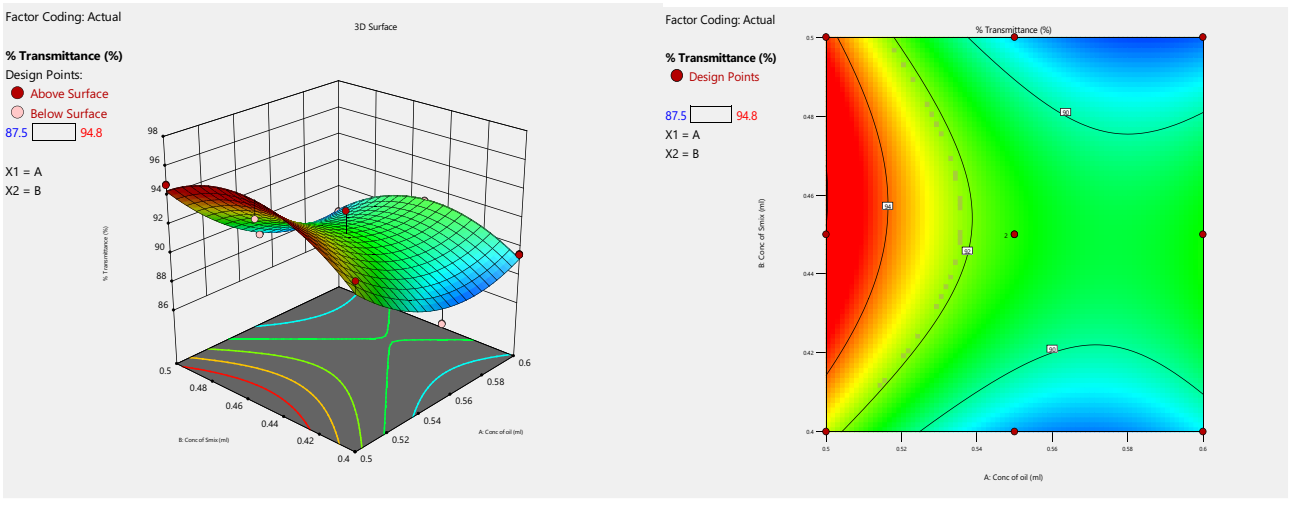

(a) (b)

Figure 3 (**a**) 3D response graph and (**b**) contour plot for the effect of concentration of eucalyptus oil and surfactant: cosurfactant (S_{mix}) on % transmittance shows that as S_{mix} concentration raised, the % transmittance also increased and decreased with eucalyptus oil concentration increased.

$$Y_2(\%\ T) = 91.34 - 2.36X_1 + 0.2500X_2 - 0.7250X_1X_2 + 2.27X_1^2 - 2.49X_2^2 \quad (4)$$

Effect of X_1 and X_2 on ET

As stated earlier, ET was an important factor in optimizing the RL-SNEDDS after dispersing into water. RL-SNEDDS formulation batches of F3, F4, F7, and F9 required less time for dispersion, which indicated the formulation had nanosized globules. In addition, the visual observation of all of these batches showed a transparent bluish-tint appearance. From equation 5, it can be indicated that the quadratic interactive models with adjusted and the predicted R^2 value was near about one for the %T. Figure 4 indicates the influence of eucalyptus oil and S_{mix} on the time of emulsification. All batches showed emulsification times within a minute. It can be inferred that the emulsification time decreased with the increased concentration of S_{mix} and the emulsification time increased with increased oil concentration.

$$Y_3(ET) = 53.43 + 5.17\ X_1 - 1.33\ X_2 - 6.25\ X_1X_2 - 8.36\ X_1^2 + 4.14\ X_2^2 \quad (5)$$

Optimization of RL-SNEDDS Formulation

Following an analysis of the impact of independent variables on the dependent factors, the study ascertained the ideal values for these variables to get the best results. The second-order polynomial equations with positive and negative sign terms confirmed the favorable and inverse relation between the concentration of eucalyptus oil and S_{mix} with all responses. The optimum RL-SNEDDS formulation's dependent variables like low ET, smaller DS, and higher %T were obtained by decreasing oil concentrations and increasing S_{mix} concentrations. The values of these factors that resulted in the best results were found after an examination of how the independent variables affected the responses. The optimized region for dependent variables was shown in Figure 5. Hence, the F7 batch was considered as an optimized batch having DS 129.3 ± 1.57 nm with PDI 0.12 ± 0.003, %T 94.82 ± 0.61, with ZP −24.6 ± 0.34 mV as shown in Figure 6 and Table 3. The % DR and % EE of the F7 batch were also determined and found to be 98.86 ± 0.23% and 97.74 ± 0.72% respectively with an emulsification time of 42 ± 1sec.

Characterization of Optimized RS-SNEDDS Formulation

The conventional liquid RL-SNEDDS have some limitations related to stability. Subsequently, eucalyptus oil causes irritation effect to the mouth. Therefore, it needs to suppress the irritation effect of eucalyptus and also provide stability.

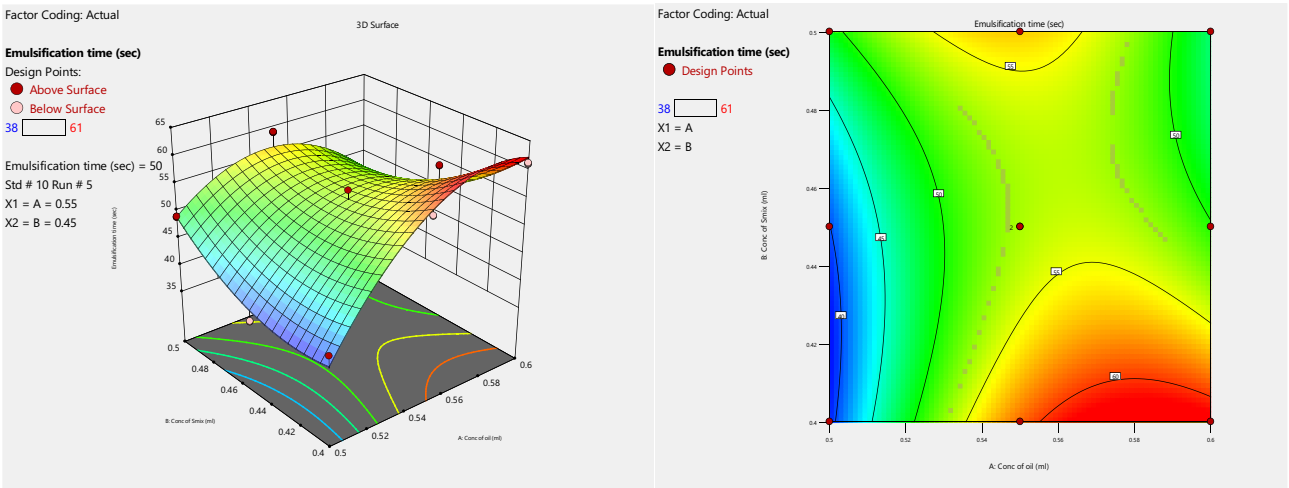

(a) (b)

Figure 4 (**a**) 3D response graph and (**b**) contour plot for the effect of concentration of eucalyptus oil and surfactant: cosurfactant (S_{mix}) on emulsification time shows that the emulsification time decreased with the increased concentration of S_{mix} and the emulsification time increased with increased oil concentration.

https://doi.org/10.2147/IJN.S499024

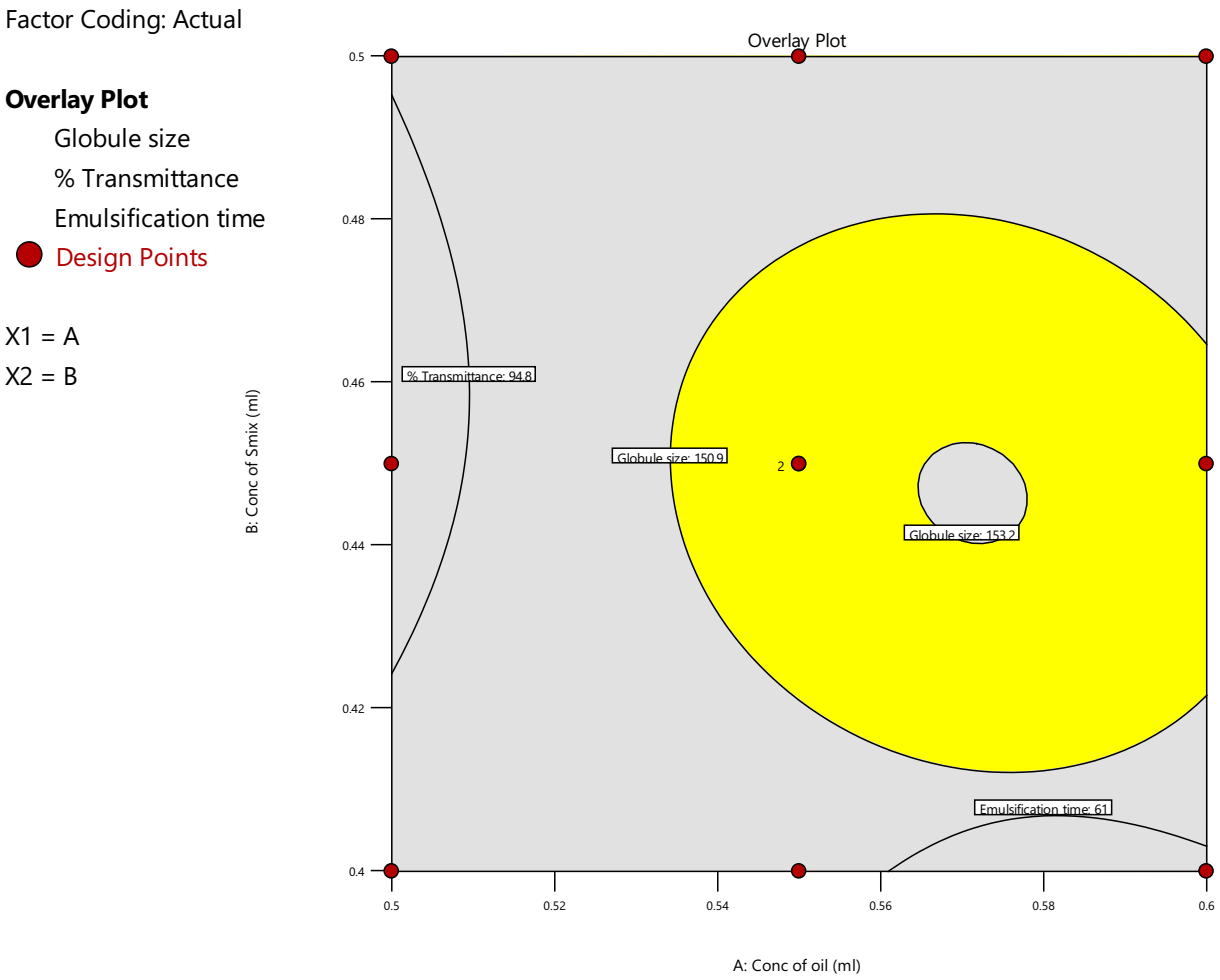

Figure 5 Overlay plot of all independent variables effect including the concentration of eucalyptus oil and surfactant: cosurfactant (S_{mix}) to confirm the optimized batch of RL-SNEDDS. The yellow region showed the optimized region of the nanoemulsion.

Therefore, the optimized F7 batch of RL-SNEDDS was lyophilized and transformed to RS-SNEDDS using mannitol as an adsorbent.

DS, PDI, ZP, %DL and %EE Determination

The formulated RS-SNEDDS indicated %EE 97.24 ±1.73% and %DL 98.37± 1.05%. The DS of RS-SNEDDS formulation was 142.3± 1.67 nm with PDI 0.21± 0.001 as shown in Figure 7a, which was slightly higher than liquid RL-SNEDDS. It might be due to the osmotic de-swelling of the RL-SNEDDS globules or the formation of ice crystals in RS-SNEDDS. However, slight aggregation of RS-SNEDDS particles recombines into larger globules. In addition to this, the coating of mannitol on the surface of RL-SNEDDS also causes a small increase in the particle size of S-SNEDD.[36] However, another peak within a range of 10–100nm particle size was formed due to erosion and polymeric disentanglement due to the shearing of particles at drying. ZP of RS-SNEDDS was shown to be 23.4 ± 1.06mV the same as that of RL-SNEDDS (Figure 7b). The higher negative zeta potential value confirmed the stability of the nanoparticle due to electrostatic repulsion between the particles and less ability of aggregation.[37,38]

FTIR, DSC, and XRD Analysis

RS-SNEDDS was also evaluated for FTIR, DSC, and XRD to conform to the functional group interaction and phase transformation of rhein. The rhein entrapment in eucalyptus oil and the formation of hydrogen bonds with the hydroxyl

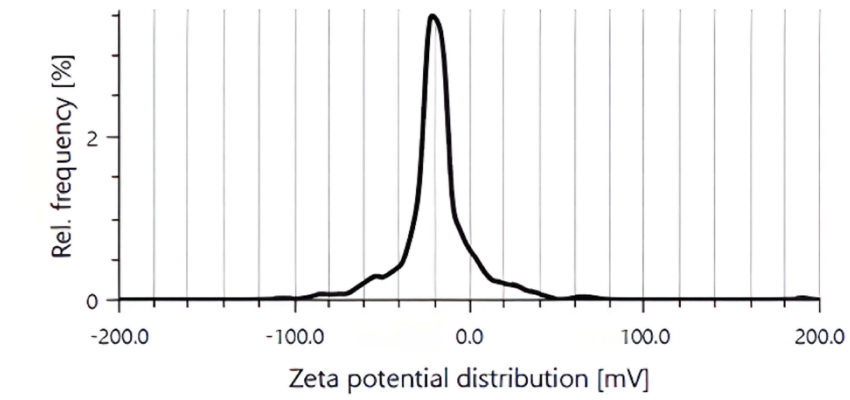

(a)

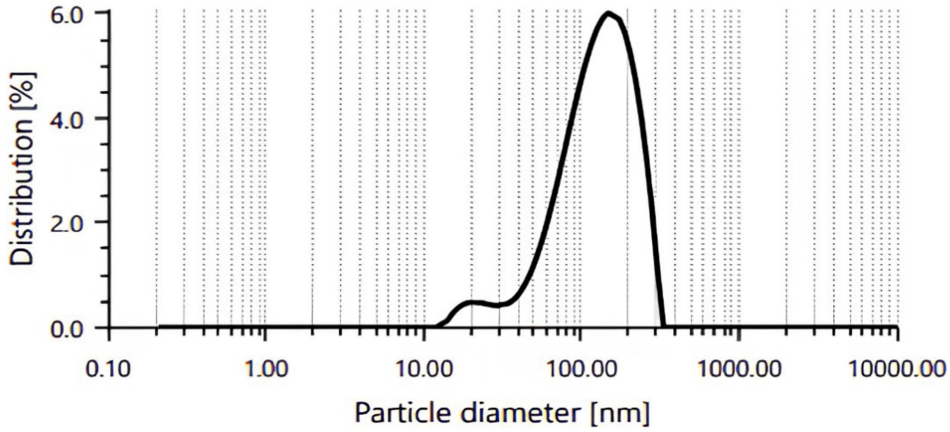

(b)

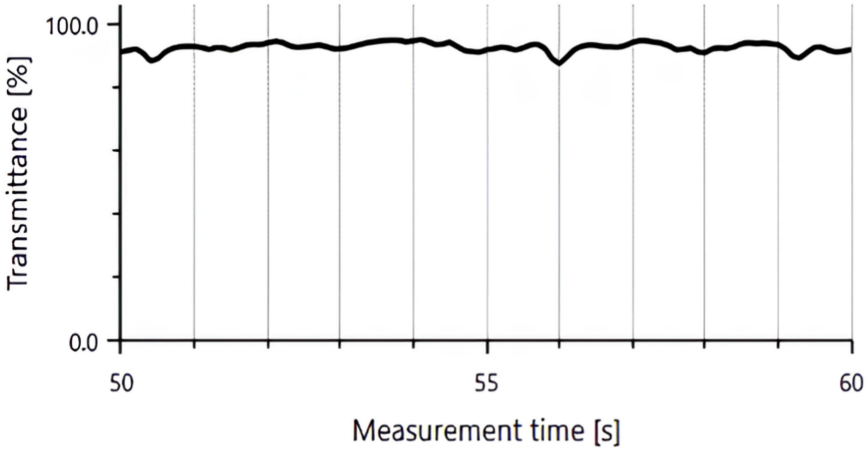

(c)

Figure 6 (**a**) Zeta potential −24.6mV±0.34 which confirms the stability of emulsion droplets (**b**) droplet size, 129.3±1.57nm showed enhanced total surface area which helped to increase the drug release and (**c**)% transmittance 94.82± 0.61 showed confirmation of emulsion in nanometric size of the optimized batch of rhein-loaded liquid nanoemulsion (RL-SNEDDS) (F7).

group of PEG-400 confirm the cross-linking linking which increases the solubility and dissolution rate of rhein through RS-SNEDDS. The FTIR spectrum of rhein, RL-SNEDDS, and RS-SNEDDS was represented in Figure 8. The intensity of sharp aromatic =C-H peak of rhein at 3061 cm^{-1} was significantly decreased in RL-SNEDDS. The C-H bending of

https://doi.org/10.2147/IJN.S499024

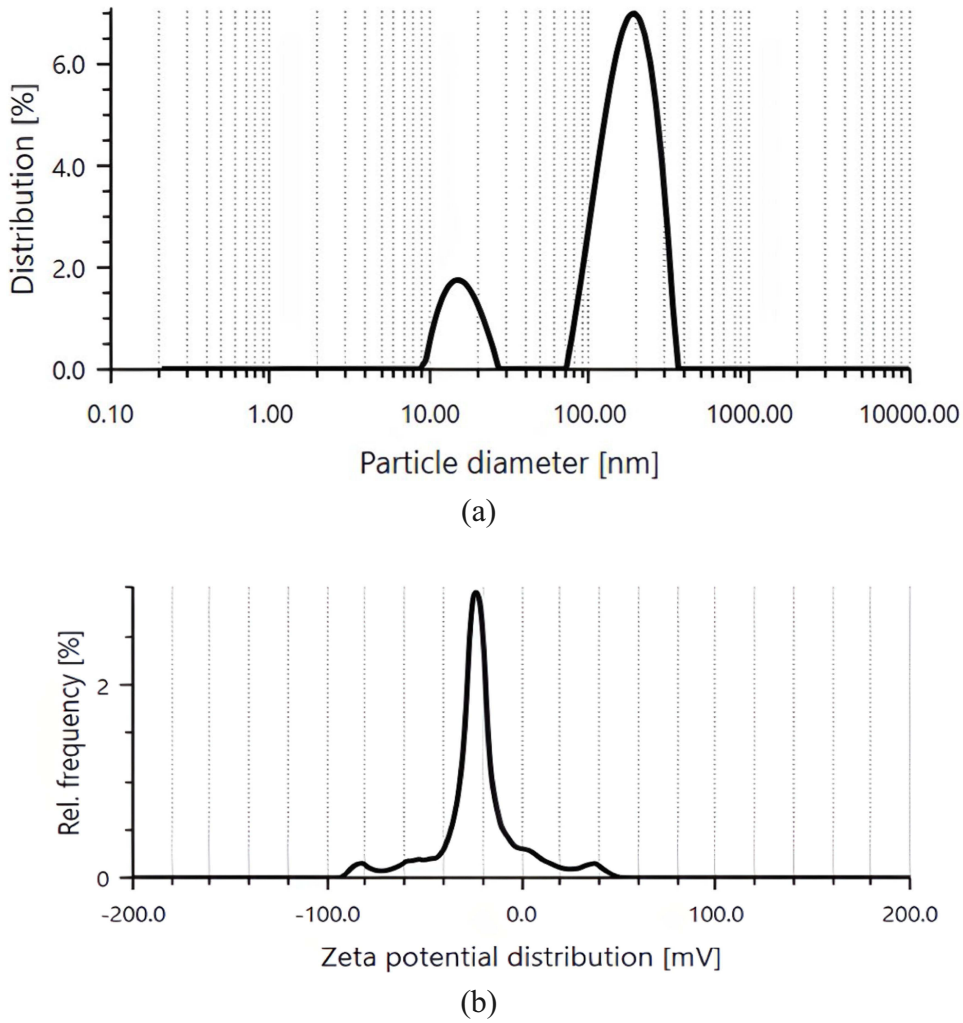

Figure 7 (**a**) Particle size of rhein-loaded solid nanoemulsion (RS-SNEDDS) was 142.3±1.67nm with polydispersity index 0.21±0.001 confirming the nanoparticle size and uniformity of particles after solidification and (**b**) zeta potential −23.4±1.06mV confirming the nanocarrier stability.

rhein was shifted from 750 cm^{-1} to 761 cm^{-1} and aromatic C=C stretch shifted from 1629 cm^{-1} to 1633 cm^{-1} with the decrease in intensity and area in RL-SNEDDS, which designates that hydrophobic interaction in between eucalyptus oil and rhein. Broadening of the IR band from 3600 cm^{-1} to 3000 cm^{-1} in RL-SNEDDS indicates the formation of hydrogen bonds due to cross-linking between the phenolic hydroxyl group and carboxylic group of rhein with PEG-400 and mannitol. The C-O stretch of the carboxylic acid shift from 1267 cm^{-1} to 1247 cm^{-1} showed the physical interaction of the bioactive rhein with PEG-400, which helps to enhance solubilization. It was suggested that rhein forms a complex with eucalyptus oil and S_{mix} after its entrapment.[39–41] However, the functional groups peak of IR for aromatic =C-H peak, and C-H bending was significantly mixed with others and formed a broad peak at 3385.07 and 723.31cm^{-1} in RS-SNEDDS due to phase transition and interaction with mannitol.

The sharp endothermic characteristic peak of rhein at 332.6°C in DSC analysis confirmed the melting point and crystalline nature of rhein. The sharp endothermic peak at 162.4°C in RS-SNEDDS corresponds to the melting point of mannitol. The DSC analysis of rhein in RS-SNEDDS also revealed a broad peak in the presence of eucalyptus oil and S_{mix} indicating the interaction of rhein with eucalyptus oil and S_{mix} as shown in Figure 9. In the formulation, a broad exothermic peak confirmed the cross-linking of rhein with PEG-400 in presence of eucalyptus oil.[42]

The crystallinity transformational changes of rhein were observed by comparing the X-ray diffraction pattern of rhein, mannitol, and RS-SNEDDS as seen in Figure 10. The XRD pattern of RS-SNEDDS explores the phase transformation of rhein due to entrapment of rhein in eucalyptus oil and formation of hydrogen bond with the hydroxyl group of PEG-400

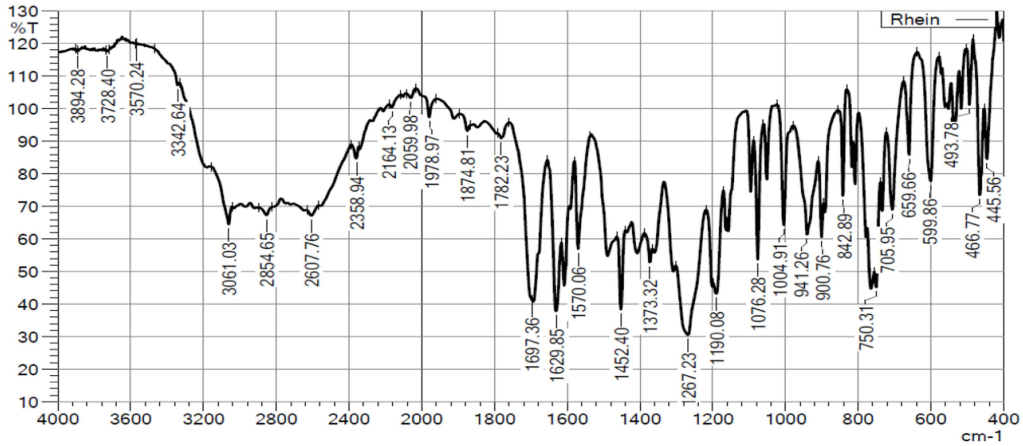

(a)

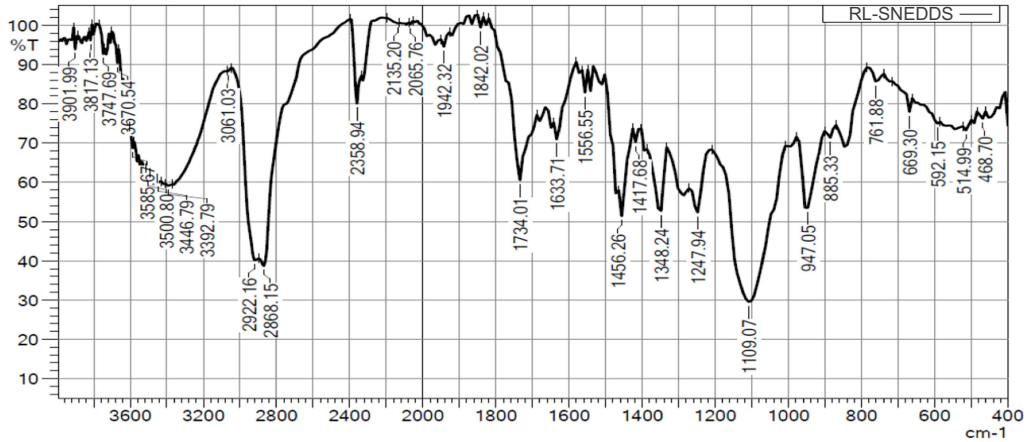

(b)

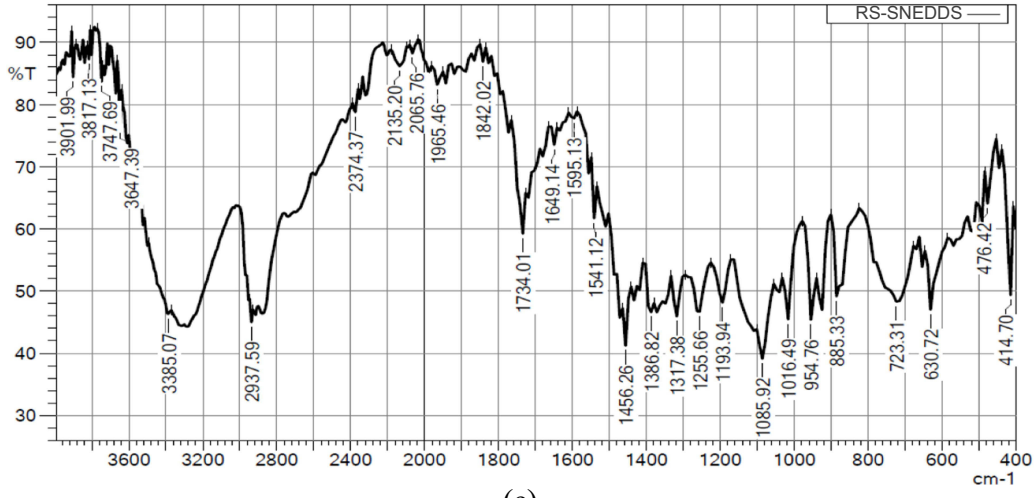

(c)

Figure 8 Fourier Transform Infrared Spectroscopy of (**a**) rhein, (**b**) rhein-loaded liquid nanoemulsion (RL-SNEDDS), and (**c**) rhein-loaded solid nanoemulsion (RS-SNEDDS) confirm the hydrophobic interaction of rhein with eucalyptus oil and PEG-400 forms a complex with eucalyptus oil and S_{mix} after its entrapment and helps to enhance solubilization.

https://doi.org/10.2147/IJN.S499024

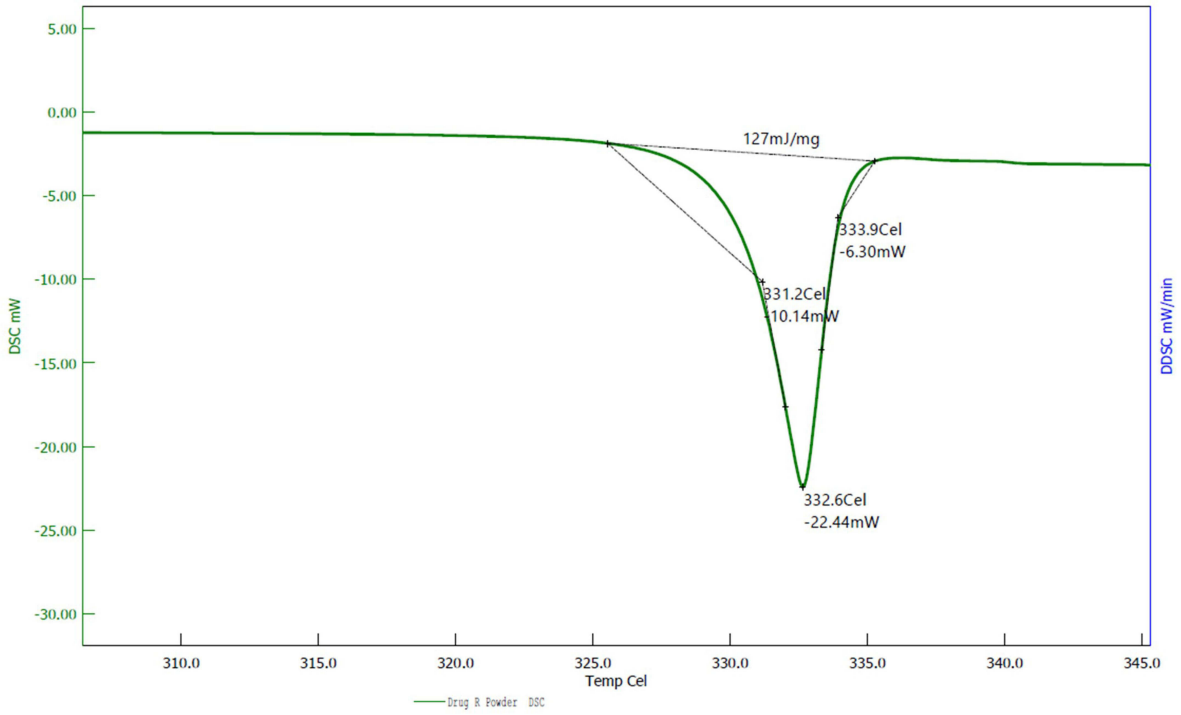

(a)

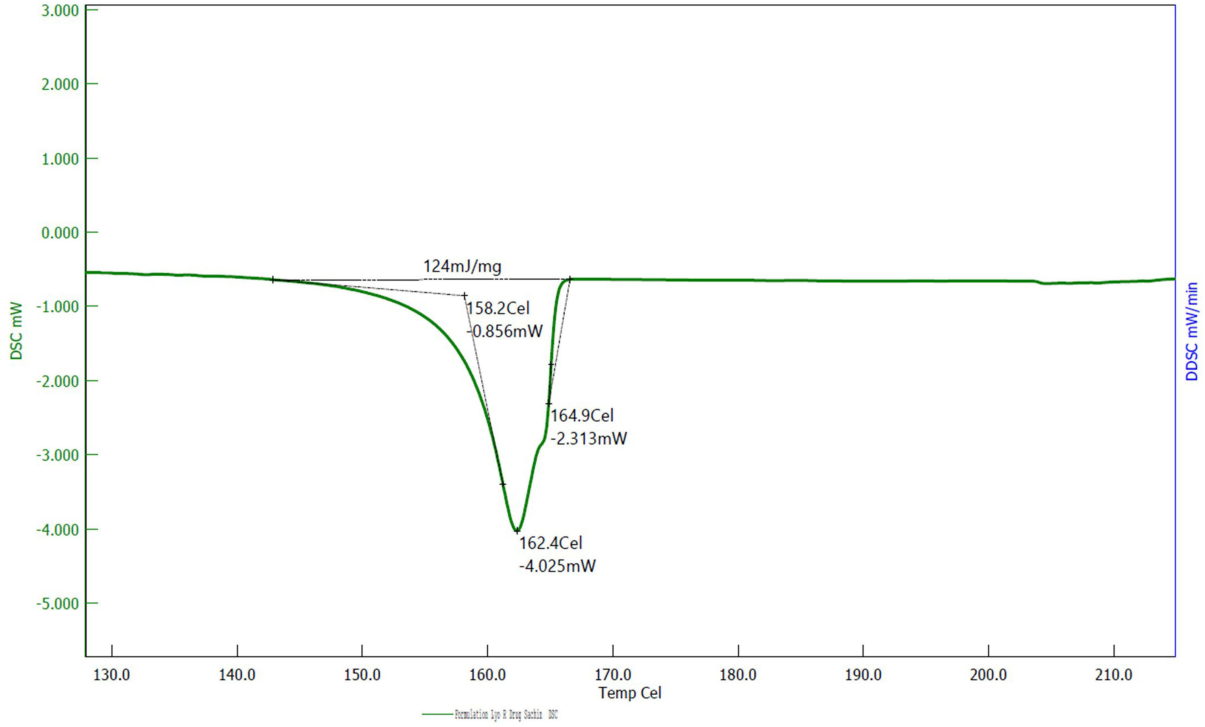

(b)

Figure 9 (**a**) Differential scanning calorimetry of rhein observed the crystalline nature of rhein and the broad peak in (**b**) Differential scanning calorimetry of rhein-loaded solid nanoemulsion (RS-SNEDDS) confirmed the cross-linking of rhein with PEG-400.

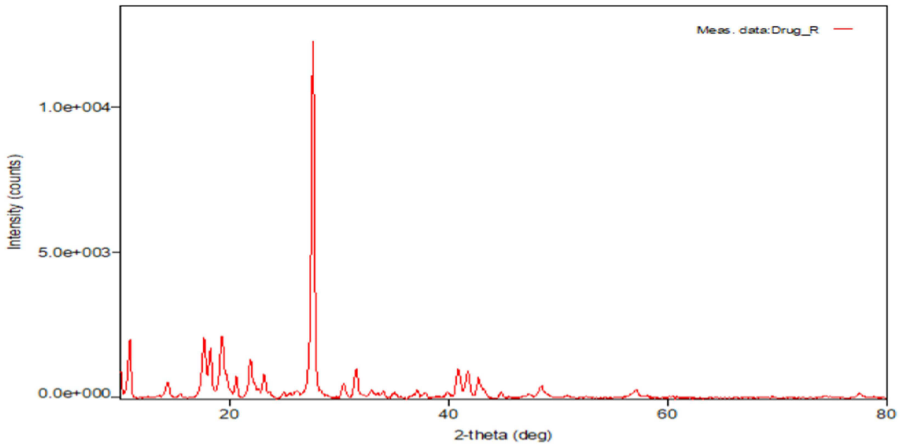

(a)

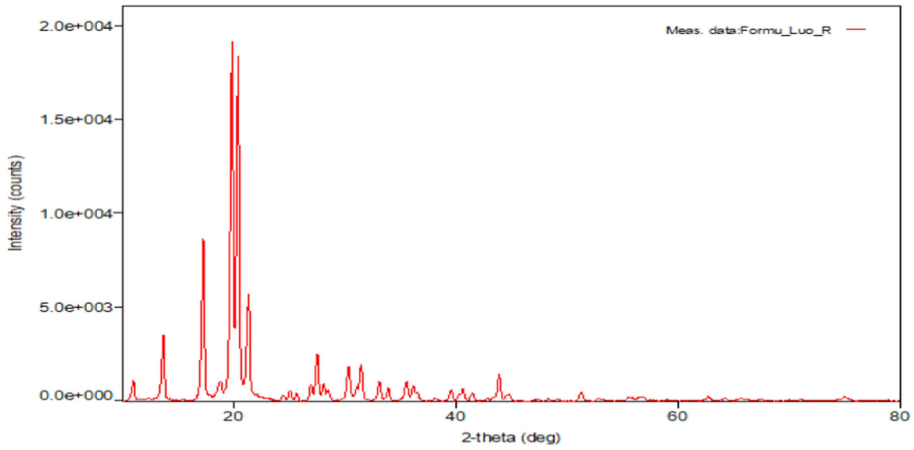

(b)

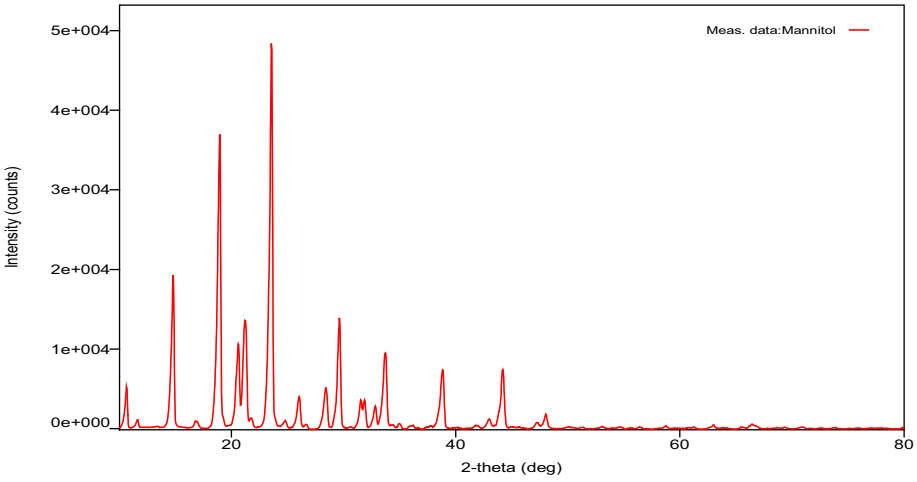

(c)

Figure 10 Powdered X-ray diffraction of (**a**) pure rhein showed the sharp and intense diffractogram peak at 2θ of 29° however, it changes to a broad peak with considerable reduction in peak intensity in (**b**) rhein-loaded solid nanoemulsion (RS-SNEDDS). It indicated the complete amorphism of free rhein and confirmed the phase transition of rhein, which helps to enhance the solubility of Rhein. The intense diffractograms of (**c**) mannitol at 2θ of 20° and 23° also found in RS-SNEDDS due to the adsorption of mannitol.

https://doi.org/10.2147/IJN.S499024

in the formulation. The pure rhein showed the sharp and intense diffractogram peak at 2θ of 29°; however, it changes to a broad peak with considerable reduction in peak intensity in RS-SNEDDS. It indicated the complete amorphism of free rhein, which helps to enhance the solubility of rhein.[43,44] The intense peak at 2θ of 20° and 23° in RS-SNEDDS was observed due to the adsorption of mannitol.

FE-SEM Analysis

The particle size and surface morphology were confirmed through FE-SEM. FE-SEM of rhein-loaded RS-SNEDDS revealed the smooth surfaced spherical particles of uniform size with a nano-sized range of 140–160nm as shown in Figure 11. The adsorption of mannitol revealed slight aggregation of RL-SNEDDS particles. The nanometric size range

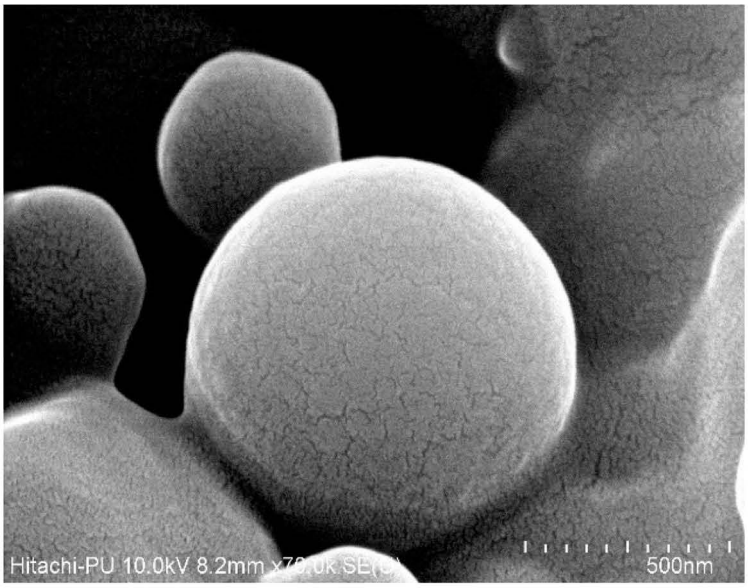

(a)

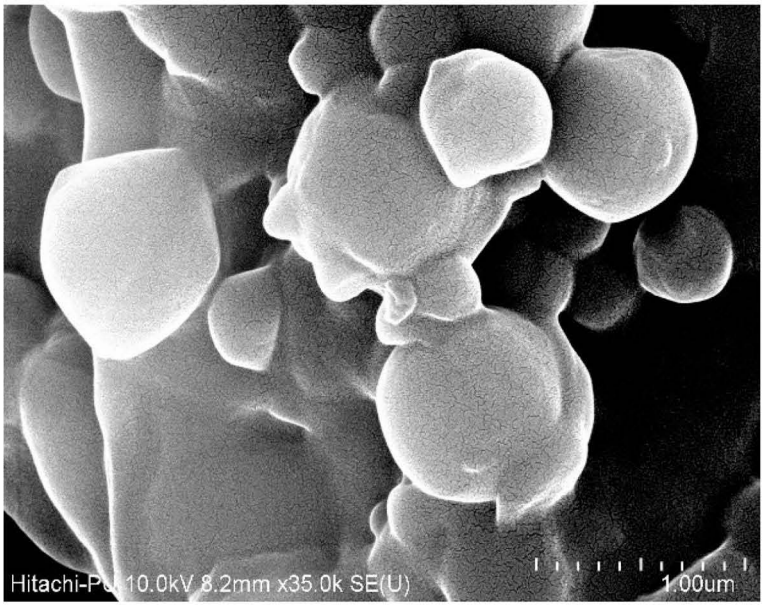

(b)

Figure 11 Field emission scanning electron microscopy image of (**a**) rhein-loaded solid nanoemulsion (RS-SNEDDS) confirmed the nano-size and morphology of RS-SNEDDS and (**b**) slight aggregation of particles due to the surface coating of mannitol which showed cross-linking with PEG-600.

significantly increases the surface area which helps to enhance dissolution rate. It also helps to decrease the diffusion layer thickness which supports to increase in the drug release rate and ultimately enhances absorption.[45]

In vitro Dissolution Study and Release Kinetics

The results revealed that RL-SNEDDS showed 85.16 ± 1.24 and 92.09 ± 1.21% release of rhein at pH 4 and 6.8, respectively, within 120 min. RS-SNEDDS showed 91.52 ± 2.01 and 98.18 ± 1.04% cumulative percentage drug release within 120 min at pH 4 and 6.8. Free rhein showed only 21% and 23% cumulative percentage drug release due to less solubility as shown in Figure 12a and b. The performance of rhein release from RL-SNEDDS and RS-SNEDDS was less at acidic pH 4 as compared to neutral pH 6.8. It was generally acknowledged that the hydroxyl group of S_{mix} encourages the release of rhein at neutral pH as compared to acidic pH.[42] The performance of rhein release from RL-SNEDDS and RS-SNEDDS was due to DS. According to the literature, the surface area is inversely proportional to DS, and drug dissolution is directly related to the surface area, ultimately facilitating drug release.[39] Thus, RL-SNEDDS and RS-SNEDDS observed enhanced rhein release due to small DS with greater surface area. Initially, a low dissolution rate was found in RS-SNEDDS as compared to RL-SNEDDS because the DS of RS-SNEDDS was slightly greater due to the adsorption of mannitol. Furthermore, the dissolution of the adsorbed mannitol layer of RS-SNEDDS decreases the

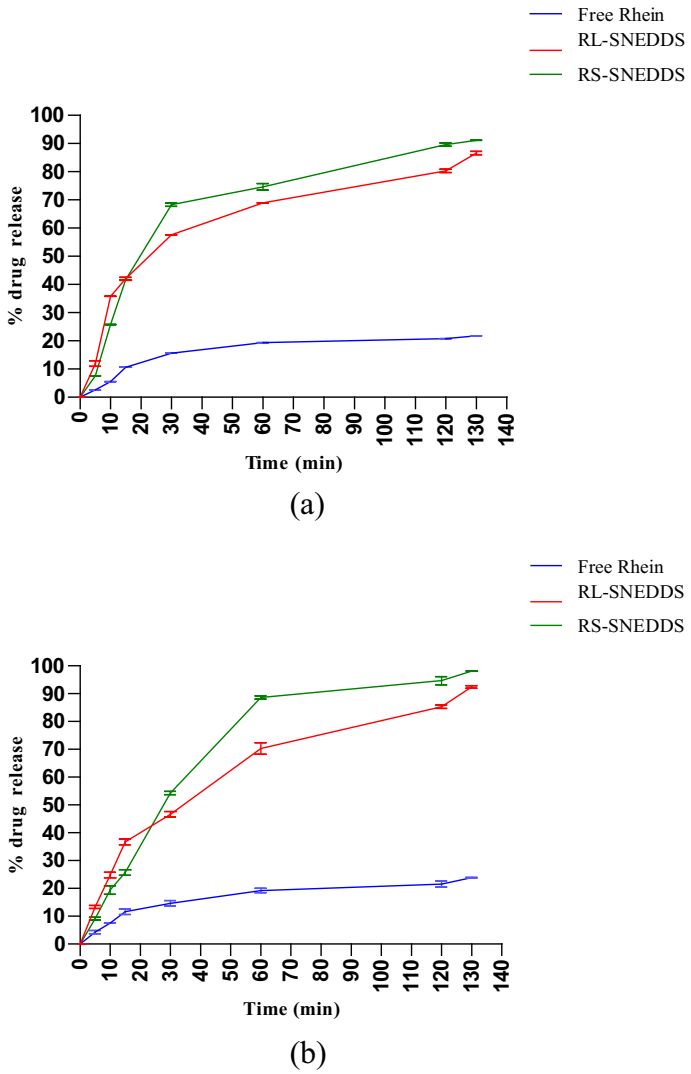

Figure 12 In-vitro %cumulative drug release of Rhein at (**a**) pH 4 and (**b**) pH 6.8 from free rhein, rhein-loaded liquid nanoemulsion (RL-SNEDDS), and rhein-loaded solid nanoemulsion (RS-SNEDDS) (All values are represented as mean ± SD (n= 3).

https://doi.org/10.2147/IJN.S499024

thickness of the diffusion layer and particle size. In addition, the dissolved form of rhein in eucalyptus oil, and S_{mix} supports enhancing the release rate of rhein at pH 6.8 as compared to free rhein. It might help to enhance absorption from the region of the small intestine and increase oral bioavailability.[18,40] Since rhein was placed in the core of eucalyptus oil and S_{mix} nano-emulsion globules helped to reduce the gastric irritation potential.[42] PEG-400 was acting as a co-surfactant in the formulation of RL-SNEDDS and RS-SNEDDS which was widely used for increasing the solubility of rhein with the help of surfactant tween 80. As reported by Yuan et al the in vitro dissolution study of rhein-loaded poly (lactic-co-glycolic acid) NPs had slow-release characteristics (70% of rhein was released within 5 hours) which was due to the strong hydrophobic interaction between polymer and drug. The drug release behavior from these NPs was best fitted to the Higuchi release kinetics model that revealed rhein could be controlled release from NPs.[46] These results are in good agreement with our results.

The dissolution data of RL-SNEDDS and RS-SNEDDS for pH 4 and 6.8 were fitted into various kinetic models as shown in Table 4 and Table 5 and determined their release kinetics. Free rhein and RL-SNEDDS followed the Higuchi release kinetics at both pH 4 and 6.8. It indicated that rhein was released by diffusion. However, RS-SNEDDS followed Hixon Crowell, which showed that the dissolution rate changed with particle size and related surface area. The n value which designates the release exponent in the release kinetic was near about 0.5 for RL-SNEDDS formulation at both pH as shown in Table 4 and Table 5. It suggests that RL-SNEDDS followed the Fickian diffusion which showed an initially greater rate of dissolution. In contrast, the n value in RS-SNEDDS was greater than 1 showing super case II transport. Pure rhein also showed a value of n = 0.5231 and 0.5181 at pH 4 and 6.8, respectively, which followed Fickian diffusion.[47] When state transitions and stresses combine with a drug transport it shows erosion and polymeric disentanglement in a hydrophilic polymer and an increased rate of dissolution.[48]

Bioanalytical Method Development and Validation

The concentration of rhein was determined using a simple and sensitive RP-HPLC bioanalytical technique. The developed optimized method of RP-HPLC comprised an aqueous solution of orthophosphoric acid pH 3 (pump A), and acetonitrile (pump B) in a 45:55 ratio with a 1.2 mL/min, flow rate for fifteen minutes. The rhein and IS was resolved at retention times 9.2 ± 0.032 and 6.8 ± 0.021mins, respectively, at 250 nm. All resolution parameters like resolution factor, capacity factor, number of theoretical plates, tailing factor, and HETP were found to be as per compliance with ICH guidelines and related to rhein and IS were confirmed by the ICH guidelines[29] (1S-a, Table S1 and Figure S1). The developed analytical method

Table 4 Comparison of Release Rate Kinetics of Rhein from Free Rhein, RL-SNEDDS, and RS-SNEDDS at pH 4

Sr.No	Formulation	Zero-order (R^2)	First order (R^2)	Higuchi (R^2)	Hixon Crowell cube root (R^2)	Rhein release exponent (n)
1	Free Rhein	0.6041	0.7811	0.97101	0.8876	0.5231
2	RL-SNEDDS	0.8204	0.7829	0.9804	0.8879	0.5186
3	RS-SNEDDS	0.7314	0.8163	0.9521	0.9841	1.9273

Table 5 Comparison of Release Rate Kinetics of Rhein from Free Rhein, RL-SNEDDS, and RS-SNEDDS at pH 6.8

Sr.No	Formulation	Zero-order (R^2)	First order (R^2)	Higuchi (R^2)	Hixon Crowell cube root (R^2)	Rhein release exponent (n)
1	Free Rhein	0.7212	0.8101	0.9831	0.8827	0.5181
2	RL-SNEDDS	0.6834	0.8124	0.9894	0.8617	0.5021
3	RS-SNEDDS	0.7429	0.8925	0.9521	0.9862	2.1203

was also specific to determining rhein in plasma samples, which was determined using the peak purity threshold and its index (1S-b, Figure S2). The investigation on linearity was carried out throughout a range of concentrations of 1µg/mL-5 µg/mL in plasma (1S-c, Figure S3a and S3b). The LOQ was 12 ng/mL and the lower LOD was 7 ng/mL accordingly. It confirmed that the optimized technique was very sensitive to quantifying the lowest concentration of rhein (1S-d). The extraction recovery and matrix effect for rhein in plasma samples at concentrations 0.05µg/mL, 0.5µg/mL, and 5 µg/mL were 85.78–89.03% and 94.78–103.43%, respectively (1S-e, Table S2). Intra-day and inter-day precision and accuracy results were found within the acceptable limit of ±15% coefficient of variation (1S-f, Table S3). These validation results demonstrated that the method is robust and fits the requirements of the pharmacokinetic investigation.

Plasma and Brain Tissue Pharmacokinetics

A single dose of free rhein and RS-SNEDDS equivalent to 10mg/Kg of rhein was administered orally to male Sprague-Dawley rats, and drug plasma concentration was estimated by non-compartmental analysis. The total area under the curve (AUC) of RS-SNEDDS was calculated about free rhein to establish its relative bioavailability. Other pharmacokinetic characteristics, including half-life ($t_{1/2}$) and clearance (Cl), were then determined and reported in Table 6.

The documented results revealed that the absorbance of the RS-SNEDDS formulation potentially improved the relative oral bioavailability of rhein. Surface charge and DS impacted RL-SNEDDS's subsequent biodistribution and blood clearance. Therefore, the nanosized and cationic charged RS-SNEDDS would improve the pharmacokinetic behavior of rhein by sustained release up to 24 hrs as shown in Figure 13a. According to the literature, RL-SNEDDS is mostly absorbed by enterocytes and gut-associated lymphoid tissues. Following that, the drug was slowly released, increasing mean residence time (MRT) and AUC0-t, hence increasing the oral bioavailability of rhein.[49] The significantly increased maximum concentration (C_{max}) (5.08 µg/mL), $t_{1/2}$ (3.84 hrs), and decreased Cl (0.32 µg/mL) for rhein through RL-SNEDDS showed decreased gastric degradation and bypass first-pass metabolism. This helps to improve blood circulation and prolong the release of rhein as compared to free rhein as shown in Table 6. Our results agree with the reported work by Yuan et al. He reported that the $AUC_{0-\infty}$ of rhein-loaded poly (lactic-co-glycolic acid) NPs was 3.7 times higher than that of drug suspension suggesting that rhein NPs had absorbed mostly over 12 hours. The NPs also significantly prolonged the $t_{1/2}$, increased the MRT, and thereby enhanced the bioavailability.[46]

The tissue distribution study expressed that, all pharmacokinetic parameters such as MRT, time to reach (T_{max}), C_{max}, $t_{1/2}$, and AUC_{0-t} were also significantly increased in brain tissue as compared to free rhein as shown in Table 6 and Figure 13b. The C_{max} and AUC of RS-SNEDDS in plasma were found to be 8 ± 0.930 µg/mL and 37.79 ±2.01 µg/mL *hr. However, the C_{max} and AUC of free rhein were found to be 1.96 ± 0.712 µg/mL and 7.32 ± 0.946 µg/mL*hr, respectively. It confirmed the significant increase in the bioavailability of rhein through RS-SNEDDS as compared to free

Table 6 Comparison of All Pharmacokinetic Parameters by Oral Administrating Free Rhein and RS-SNEDDS in Plasma and Brain Tissue

Parameter	Plasma		Brain	
	Free rhein	RS-SNEDDS	Free rhein	RS-SNEDDS
$t_{1/2}$ (hrs)	1.64±0.821	3.84±0.412$^{\#}$	1.36±0.240	2.92±0.102$^{\#\#}$
T_{max} (hrs)	1.00	2.00	3.00	4.00
C_{max} (µg/mL)	1.96±0.712	5.08±0.930$^{\#}$	0.68±0.003	2.90±0.171$^{\#}$
AUC_{0-t} (µg/mL*hr)	7.32±0.946	37.79±2.013$^{\#}$	2.64±0.091	18.18±1.68$^{\#}$
MRT (hrs)	3.57±0.912	6.50±0.830$^{\#}$	4.39±0.472	6.50±0.931$^{\#\#}$
Vz/F (µg/mL)	2.06±0.723	1.49±0.042	7.37±0.894	2.30±0.103
Cl/F (µg/mL)/hrs)	1.29±0.0826	0.32±0.002$^{\#}$	3.75±0.002	0.54±0.001$^{\#}$

Note: All values are represented as mean ± SD (n= 3). $^{\#}$ $p<0.001$ compared to the free rhein group. $^{\#\#}$ $p<0.01$ compared to the free rhein group.

https://doi.org/10.2147/IJN.S499024

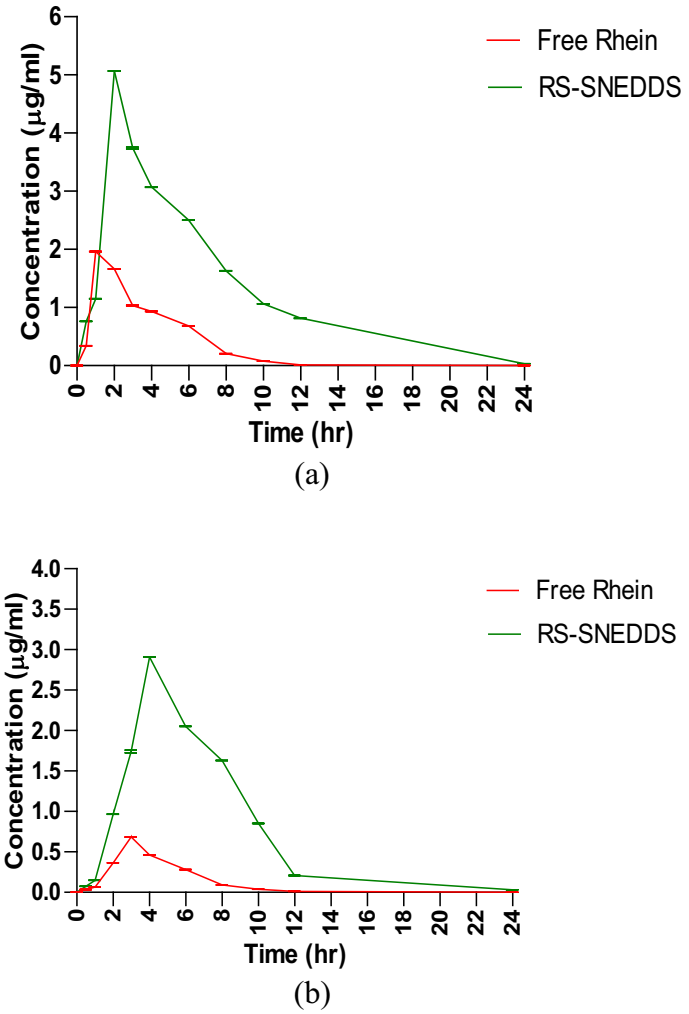

Figure 13 (**a**) Plasma and (**b**) brain tissue pharmacokinetics after oral administration of free rhein and rhein-loaded solid nanoemulsion (RS-SNEDDS) (All values are represented as mean ± SD (n = 3)) confirmed the enhanced mean residence time (MRT) and total area under the curve (AUC_{total}) which ultimately increased the oral bioavailability of the rhein.

rhein. Subsequently, the C_{max} and AUC of rhein through RS-SNEDDs were found to be 2.90 ± 0.171 µg/mL and 18.18 ± 1.68 µg/mL*hr in brain tissue, which also confirmed its potential therapeutic efficacy in CNS disorder. From plasma and brain pharmacokinetic data, the absorption behavior of RS-SNEDDS was confirmed through the bypass of the encapsulated rhein from gastric and intestinal degradation. Subsequently, it increases the possible uptake and transport through intestinal mucosa, which helps to increase oral bioavailability.[8] The plasma and brain tissue pharmacokinetic results of RS-SNEDDS support the literature. Therefore, increasing the oral bioavailability and therapeutic efficacy of rhein through RS-SNEDDS in CNS disorders was suggested.

Conclusion

The present study highlights the development and optimization of rhein-loaded SNEDDS to improve its biopharmaceutical performance. Rhein-loaded SNEDDS was successfully formulated based on the higher solubility of rhein in eucalyptus oil, and the better emulsifying ability of tween 80: PEG 400 (3:1), and optimization was performed using 3^2 factorial designs. The optimized batch was selected based on response surface methodology and desirability function. The optimized SNEDDS was lyophilized and transformed to RS-SNEDDS using mannitol for improved stability and ease of handling. RS-SNEDDS observed a globule size of 142.3 ± 1.67 nm with PDI 0.21± 0.001 and a high entrapment efficiency of 97.24 ±1.73%. The Zeta potential of RS-SNEDDS was found −23.4 ± 1.06mV which restricts golubule

aggregation and enhances stability. Rhein significantly increased the dissolution rate through RS-SNEDDS as compared to free rhein by following the Hixson Crowell mechanism. Solid-state characterization of RS-SNEDDS showed the amorphous nature of rhein in the formulation. The C_{max} and AUC of RS-SNEDDS in plasma were found to be 8 ± 0.930 µg/mL and 37.79 ±2.01 µg/mL *hr whereas, the C_{max} and AUC of free rhein were found to be 1.96 ± 0.712 µg/mL and 7.32 ± 0.946 µg/mL*hr, respectively, which confirmed the significant increase in the bioavailability of rhein through RS-SNEDDS as compared to free rhein. Subsequently, the C_{max} and AUC of rhein through RS-SNEDDs were found to be 2.90 ± 0.171 µg/mL and 18.18 ± 1.68 µg/mL*hr in brain tissue which also confirmed its potential therapeutic benefits in CNS disorder. Therefore, this study concludes that the RS-SNEDDS formulation is a promising delivery platform for improving oral bioavailability. However, this study further required a detailed investigation of pharmacodynamic evaluation in animal models and efficacy in humans.

Institutional Review Board Statement

The animal study protocol was approved by the Institutional Animal Ethics Committee (IAEC) of Dadasaheb Balpande College of Pharmacy, Nagpur, India, with approved protocol number DBCOP/IAEC/1426/2022-23/P11. This study was performed according to the guidelines of the Committee for the Purpose of Control and Supervision Experiments on Animals (CPCSEA), Ministry of Social Justice and Empowerment, Government of India.

Data Sharing Statement

All generated and analyzed data have been incorporated into the manuscript.

Acknowledgments

The authors extended their appreciation to the Deanship of Scientific Research at King Khalid University for funding this work through a large group research project under grant number RGP.2/537/45. The authors are also thankful for providing the opportunity to work at the Department of Pharmacology, Dadasaheb Balpande College of Pharmacy, Nagpur, India.

Disclosure

The authors declared that there was no conflict of interest.

References

1. He Z H, Zhou R, He M-F, et al. Anti-angiogenic effect and mechanism of rhein from Rhizoma Rhei. *Phytomedicine*. 2011;18:470–478. doi:10.1016/j.phymed.2010.10.006
2. Zhu Y, Yang S, Lv L, et al. Research Progress on the Positive and Negative Regulatory Effects of Rhein on the Kidney: a Review of Its Molecular Targets. *Molecules*. 2022;27:6572. doi:10.3390/molecules27196572
3. More S, Kaleem M, Kharwade R, et al. Depression unveiled: insights into etiology and animal models for behavioral assessment, exploring the multifactorial nature and treatment of depression. *Brain Res*. 2025;1847:149313. doi:10.1016/j.brainres.2024.149313
4. Li H, Guo H, Wu L, et al. Comparative pharmacokinetics study of three anthraquinones in rat plasma after oral administration of Radix et Rhei Rhizoma extract and Dahuang Fuzi Tang by high-performance liquid chromatography-mass spectrometry. *J Pharm Biomed Anal*. 2013;76:215–218. doi:10.1016/j.jpba.2012.12.004
5. Dizaj SM, Vazifehasl Z, Salatin S, Adibkia K, Javadzadeh Y. Nanosizing of drugs: effect on dissolution rate. *Res Pharm Sci*. 2015;10 2 95–108.
6. Beg S, Jena SS, Patra CN, et al. Development of solid self-nanoemulsifying granules (SSNEGs) of ondansetron hydrochloride with enhanced bioavailability potential. *Colloids Surf B Biointerfaces*. 2013;101:414–423. doi:10.1016/j.colsurfb.2012.06.031
7. Yao W, Xu Z, Sun J, et al. Deoxycholic acid-functionalised nanoparticles for oral delivery of rhein. *Eur J Pharm Sci*. 2021;159:105713. doi:10.1016/j.ejps.2021.105713
8. Feng H, Zhu Y, Fu Z, Li D. Preparation, characterization, and in vivo study of rhein solid lipid nanoparticles for oral delivery. *Chem Biol Drug Des*. 2017;90:867–872. doi:10.1111/cbdd.13007
9. Luo J, Sun J, Luo X, et al. Low molecular weight chitosan-based conjugates for efficient Rhein oral delivery: synthesis, characterization, and pharmacokinetics. *Drug Dev Ind Pharm*. 2019;45:96–104. doi:10.1080/03639045.2018.1522326
10. Mahajan N, Mujtaba MA, Fule R, et al. Self-Emulsifying Drug Delivery System for Enhanced Oral Delivery of Tenofovir: formulation, Physicochemical Characterization, and Bioavailability Assessment. *ACS Omega*. 2024 9 8139–8150. doi:10.1021/acsomega.3c08565
11. Baloch J, et al. Self-nanoemulsifying drug delivery system (Snedds) for improved oral bioavailability of chlorpromazine: in vitro and in vivo evaluation. *Med*. 2019;55 210 doi:10.3390/medicina55050210.
12. Čerpnjak K, Zvonar A, Gašperlin M, Vrečer F. Lipid-based systems as a promising approach for enhancing the bioavailability of poorly water-soluble drugs. *Acta Pharm*. 2013;63:427–445. doi:10.2478/acph-2013-0040

13. Mohd Izham MN, Hussin, Y, Aziz, MNM et al. Preparation and characterization of self nano-emulsifying drug delivery system loaded with citraland its antiproliferative effect on colorectal cells in vitro. *Nanomaterials*. 2019;9 1028 doi:10.3390/nano9071028.
14. Mujtaba MA, Gangane P, Ali A, et al. Karanjin-loaded soya lecithin-based ethosomal nanogel for the therapeutic intervention of psoriasis: formulation development, factorial design based-optimization, in vitro and in vivo assessment. *Biomed Mater*. 2024;19:055012. doi:10.1088/1748-605X/ad5e51
15. Kharwade R, Ali, N, Gangane, P et al DOE-Assisted Formulation, Optimization, and Characterization of Tioconazole-Loaded Transferosomal Hydrogel for the Effective Treatment of Atopic Dermatitis: In Vitro and In Vivo Evaluation. *Gels* 2023 9 303 doi:10.3390/gels9040303.
16. Kuncahyo I, Choiri S, Fudholi A, Martien R, Rohman A. Assessment of fractional factorial design for the selection and screening of appropriate components of a self-nanoemulsifying drug delivery system formulation. *Adv Pharm Bull*. 2019;9:609–618. doi:10.15171/apb.2019.070
17. Hu B, Gao F, Li C, et al. Rhein laden pH-responsive polymeric nanoparticles for treatment of osteoarthritis. *AMB Express*. 2020;10 158. doi:10.1186/s13568-020-01095-3
18. Biradar MM, Mehta P. Dolutegravir Loaded Solid Self-Micro-Emulsifying Drug Delivery System for Enhanced Solubility and Dissolution. 2023;15:159–168.
19. Mujtaba MA, Kaleem, M, Chaware, R et al. Development and Optimization of Proniosomal Formulation of Irbesartan Using a Box–Behnken Design to Enhance Oral Bioavailability : Physicochemical Characterization and In Vivo Assessment. *ACS Omega*. 2024:9 14 16346–16357. doi:10.1021/acsomega.3c10506
20. Sun H, Luo G, Chen D, Xiang Z. A comprehensive and system review for the pharmacological mechanism of action of rhein, an active anthraquinone ingredient. *Front Pharmacol*. 2016;7 247. doi:10.3389/fphar.2016.00247
21. Fule R, Kaleem, M, Asar, TO et al. Formulation, Optimization and Evaluation of Cytarabine-Loaded Iron Oxide Nanoparticles: from In Vitro to In Vivo Evaluation of Anticancer Activity. *Nanomaterials*. 2023;13 175 doi:10.3390/nano13010175.
22. Yi T, Wan J, Xu H, Yang X. A new solid self-microemulsifying formulation prepared by spray-drying to improve the oral bioavailability of poorly water soluble drugs. *Eur J Pharm Biopharm*. 2008;70:439–444. doi:10.1016/j.ejpb.2008.05.001
23. Kharwade R, Kazi M, Mahajan N, et al. Mannosylated PAMAM G2 dendrimers mediated rate programmed delivery of efavirenz target HIV viral latency at reservoirs. *Saudi Pharm J*. 2024;32:102154. doi:10.1016/j.jsps.2024.102154
24. Makwana V, Jain R, Patel K, Nivsarkar M, Joshi A. Solid lipid nanoparticles (SLN) of Efavirenz as lymph targeting drug delivery system: elucidation of mechanism of uptake using chylomicron flow blocking approach. *Int J Pharm*. 2015;495:439–446. doi:10.1016/j.ijpharm.2015.09.014
25. Kaleem M, Haque SE. Evaluation of Cardioprotective role of Vinpocetine in Isoproterenol-induced Myocardial Infarction in Rats. *J Pharm Res*. 2015;9:7 408–414.
26. Yin K, Feng S. Effects of particle size and surface coating on cellular uptake of polymeric nanoparticles for oral delivery of anticancer drugs. *Biomaterials*. 2005;26:2713–2722. doi:10.1016/j.biomaterials.2004.07.050
27. Ang BC, Yaacob II, Nurdin I, Brosseau C. Investigation of Fe_2O_3/SiO_2 Nanocomposite by FESEM and TEM. *J Nanomater*. 2013;2013 28. doi:10.1155/2013/980390
28. Kharwade R, Nair H, Masurkar D, et al. Formulation and Evaluation of Chronomodulated Pulsatile Drug Delivery System for Nocturnal Hyperacidity. *Res J Pharm Technol*. 2022;15:1449–1454. doi:10.52711/0974-360X.2022.00240
29. Imre S, Vlase L, Muntean DL. Bioanalytical method validation. *Rev Rom Med Lab*. 2008;10:13–21.
30. Kharwade R, More S, Suresh E, Warokar A, Mahajan N, Mahajan U. Improvement in Bioavailability and Pharmacokinetic Characteristics of Efavirenz with Booster Dose of Ritonavir in PEGylated PAMAM G4 Dendrimers. *AAPS Pharm Sci Tech*. 2022;23 177. doi:10.1208/s12249-022-02315-8
31. Nathi R, Rao SS, Sahoo S, Sunkara N, Mohan VR. Stability Indicating Rp-Hplc Method Development And Validation Of Efavirenz In Bulk And Pharmaceutical Dosage Form. *Int J Phar Bio Sci*. 2017;7:223–229.
32. Kumar G, Sharma S, Shafiq N et al, et al. Pharmacokinetics and tissue distribution studies of orally administered nanoparticles encapsulated ethionamide used as potential drug delivery system in management of multi-drug resistant tuberculosis. *Drug Deliv* 2011;18 65–73 doi:10.3109/10717544.2010.509367.
33. Smith KM, Xu Y. Tissue Sample Preparation in Bioanalytical Assays. *Bioanalysis*. 2012 4 741–749. doi:10.4155/bio.12.19
34. Parrish NF, Wilen CB, Banks LB, et al. Transmitted / Founder and Chronic Subtype C HIV-1 Use CD4 and CCR5 Receptors with Equal Efficiency and Are Not Inhibited by Blocking the Integrin α4β7 PLoS Pathog. **8(5)** e1002686 doi:10.1371/journal.ppat.1002686, (2012).
35. Kappelhoff BS, Crommentuyn KML, de Maat MMR, et al. Practical guidelines to interpret plasma concentrations of antiretroviral drugs. *Clin Pharmacokinet*. 2004;43:845–853. doi:10.2165/00003088-200443130-00002
36. Owens DE, Peppas NA. Opsonization, biodistribution, and pharmacokinetics of polymeric nanoparticles. *Int J Pharm*. 2006;307:93–102. doi:10.1016/j.ijpharm.2005.10.010
37. Jaiswal P, Aggarwal G, Harikumar SL, Singh K. Development of self-microemulsifying drug delivery system and solid-self-microemulsifying drug delivery system of telmisartan. *Int J Pharm Inves*. 2014;4:195–206. doi:10.4103/2230-973X.143123
38. Kotta S, Aldawsari HM, Badr-Eldin SM, et al. Thermosensitive Hydrogels Loaded with Resveratrol Nanoemulsion: formulation Optimization by Central Composite Design and Evaluation in MCF-7 human Breast Cancer Cell Lines. *Gels*. 2022;8 7 450. doi:10.3390/gels8070450
39. Kharwade R. Effect of PEGylation on drug uptake, biodistribution, and tissue toxicity of efavirenz-ritonavir loaded PAMAM G4 dendrimers. *Pharm Dev Technol*. 2023:28 2 1–19 doi:10.1080/10837450.2023.2173230.
40. Fadke J, Desai J, Thakkar H. Formulation Development of Spherical Crystal Agglomerates of Itraconazole for Preparation of Directly Compressible Tablets with Enhanced Bioavailability. *AAPS Pharm Sci Tech*. 2015;16:1434–1444. doi:10.1208/s12249-015-0332-y
41. Mahajan NM, Wanaskar K, Ali N, et al. Innovative Wound Healing Hydrogel Containing Chicken Feather Keratin and Soy Isoflavone Genistein: in Vivo Studies. *Gels*. 2023;9:6 462. doi:10.3390/gels9060462
42. Kamble RN, Mehta P. Development of simple HPLC method to estimate the blood plasma concentration of efavirenz in rat after oral administration. *Int J Pharm Pharm Sci*. 2015;7:7 153–156.
43. Akkewar A, Mahajan N, Kharwade R, Gangane P. Liposomes in the Targeted Gene Therapy of Cancer: a Critical Review. *Curr Drug Deliv*. 2022;20:4 350–370. doi:10.2174/1567201819666220421113127

44. Rajan R, Vasudevan D, Biju Mukund V, Jose S. Transferosome: A vesicular transdermal delivery system for enhanced drug permeation. *J Adv Pharm Technol Res*. 2011;2:3 138. doi:10.4103/2231-4040.85524
45. Magalhães J, L. Chaves L, C. Vieira A, et al. Optimization of rifapentine-loaded lipid nanoparticles using a Quality-by-Design strategy. *Pharmaceutics*. 2020;12:1 75. doi:10.3390/pharmaceutics12010075
46. Yuan Z, Gu X. Preparation, characterization, and in vivo study of rhein-loaded poly(Lactic-co-glycolic acid) nanoparticles for oral delivery. *Drug Des Devel Ther*. 2015;9:2301–2309. doi:10.2147/DDDT.S81320
47. Ahmed R, Aucamp M, Ebrahim N, Samsodien H. Supramolecular assembly of rifampicin and PEGylated PAMAM dendrimer as a novel conjugate for tuberculosis. *J Drug Deliv Sci Technol*. 2021;66:102773. doi:10.1016/j.jddst.2021.102773
48. Zhang K, Wang Q, Yang Q, et al. Enhancement of Oral Bioavailability and Anti-hyperuricemic Activity of Isoliquiritigenin via Self-Microemulsifying Drug Delivery System. *AAPS Pharm Sci Tech*. 2019;20:1–11. doi:10.1208/s12249-019-1421-0
49. Aji Alex MR, Chacko AJ, Jose S, Souto EB. Lopinavir loaded solid lipid nanoparticles (SLN) for intestinal lymphatic targeting. *Eur J Pharm Sci*. 2011;42:11–18. doi:10.1016/j.ejps.2010.10.002